

**Development of Micropatterned, Mucoadhesive, Ocular Films for the Treatment of  
Diabetic Keratopathy**

by

**Aishwarya Vasudevan**

B.S. Pharmacy, Vivekanand Education Society's College of Pharmacy, 2018

Submitted to the Graduate Faculty of  
The School of Pharmacy in partial fulfillment  
of the requirements for the degree of  
Master of Science

University of Pittsburgh

2020

UNIVERSITY OF PITTSBURGH

SCHOOL OF PHARMACY

This thesis was presented

by

**Aishwarya Vasudevan**

It was defended on

April 1, 2020

and approved by

Lisa Rohan, Ph.D., Department of Pharmaceutical Sciences, School of Pharmacy

Song Li, Ph.D., Department of Pharmaceutical Sciences, School of Pharmacy

Thesis Advisor: Vinayak Sant, Ph.D., Assistant Professor, Department of Pharmaceutical Sciences, School of Pharmacy

Copyright © by Aishwarya Vasudevan

2020

# **Development of Micropatterned, Mucoadhesive, Ocular Films for the Treatment of Diabetic Keratopathy**

Aishwarya Vasudevan, B.S.

University of Pittsburgh, 2020

## **ABSTRACT**

According to the CDC report in 2017, approximately 9.4% of the US population suffers from diabetes. The ocular manifestations of diabetes include diabetic retinopathy, glaucoma, cataract and ocular surface diseases. Research shows that around 47-64% of diabetic individuals suffer from dysfunctional corneal wound healing in the eye, known as diabetic keratopathy. The presence of free oxygen radicals, advanced glycation products and the absence of mucins in the eyes of diabetic individuals disrupts the homeostasis required for epithelial wound healing. Current treatment for corneal wound healing is mostly symptomatic and includes administration of antibiotic drops, bandage lenses, artificial tears and punctal plugs. However, these are symptom-based treatments and there remains a need for a cause-based approach. Rebamipide eye drops are used in dry eye disease in Japan because of its ability to improve mucin secretion and maintain tear film stability. Additionally, it has shown epithelial wound healing activity along with the ability to scavenge reactive oxygen species and reduce inflammation. In this study, we have fabricated micropatterned, mucoadhesive films containing rebamipide that have a sustained release of drug from the polymer matrix. We show that these thin films containing cellulose and Eudragit polymers form clear and distinct patterns of good resolution. Micropatterned films also show good tensile strength and flexibility. Cytotoxicity studies on corneal stem cells show that the 48%EPO+32%FS30D formulation has the least toxicity with a good sustained release of drug in 24 hours. We also demonstrate the higher mucoadhesive properties of micropatterned films as

compared to plain, unpatterned films on the ocular mucosa. Finally, we show the preliminary development of an ex-vivo lacrimation model of the retention of films on the sclera using enucleated porcine eyeballs.

**Keywords:** Diabetes, diabetic keratopathy, ocular surface diseases, micropatterns, mucins, Rebamipide, films

## Table of Contents

<b>Acknowledgements .....</b>	<b>x</b>
<b>1.0 Introduction.....</b>	<b>1</b>
<b>1.1 Anatomy and Physiology of the Ocular Surface.....</b>	<b>2</b>
<b>1.2 Corneal Wound Healing .....</b>	<b>4</b>
<b>1.3 Topical Ocular Drug Delivery .....</b>	<b>7</b>
<b>1.4 Barriers To Ocular Drug Delivery .....</b>	<b>10</b>
<b>1.4.1 Tear Film And Tear Turnover .....</b>	<b>10</b>
<b>1.4.2 Tight Junctions.....</b>	<b>10</b>
<b>1.4.3 Nasolacrimal Drainage .....</b>	<b>10</b>
<b>1.5 Mucoadhesive Drug Delivery .....</b>	<b>12</b>
<b>1.6 Current Treatment Options For Diabetic Keratopathy .....</b>	<b>15</b>
<b>1.7 Research Hypothesis .....</b>	<b>17</b>
<b>2.0 Materials and Methods.....</b>	<b>21</b>
<b>2.1 Materials.....</b>	<b>21</b>
<b>2.2 Methods .....</b>	<b>22</b>
<b>2.2.1 Film Preparation .....</b>	<b>22</b>
<b>2.2.2 Formulation Of Polymeric Micropatterned Films.....</b>	<b>23</b>
<b>2.2.3 Physical Characterization Of Films .....</b>	<b>24</b>
<b>2.2.3.1 Appearance.....</b>	<b>24</b>
<b>2.2.3.2 Weight and Thickness .....</b>	<b>25</b>
<b>2.2.4 Tensile Strength.....</b>	<b>25</b>

2.2.5 Cytotoxicity Of Micropatterned Films On HCLE Cells.....	27
2.2.6 In Vitro Release Of Rebamipide From Films .....	29
2.2.6.1 Drug Content Of The Films .....	29
2.2.6.2 Release Of Rebamipide From Micropatterned Films .....	30
2.2.7 Ex-Vivo Mucoadhesion Of Films On Porcine Intestinal And Ocular Tissues .....	31
2.2.8 Ex-Vivo Ocular Retention Of Micropatterned Films .....	33
<b>3.0 Results and Discussion.....</b>	<b>35</b>
3.1.1 Film Formulation .....	35
3.1.2 Polymeric Films Form Good Three-Dimensional Patterns of High Fidelity	36
3.1.3 Micropatterned Polymeric Films Show Good Mechanical Properties.....	38
3.1.4 Eudragit Containing Micropatterned Films Are Non-Toxic To The Regenerating Corneal Limbal Epithelial Cells .....	42
3.1.5 Micropatterned Polymeric Films Show A Sustained Release Of Rebamipide Over 24 Hours .....	45
3.1.6 Micropatterned Films Possess Higher Mucoadhesion To Ocular Tissues As Compared To Unpatterned Films .....	48
3.1.7 48%EPO+32%FS30D Films Are Retained On The Sclera For More Than 5 Hours In The Ex-Vivo Eyeball Model.....	53
<b>4.0 Conclusions And Future Directions .....</b>	<b>55</b>
<b>Bibliography .....</b>	<b>58</b>

## List of Tables

<b>Table 1 Methods for improving retention of ocular dosage forms.....</b>	<b>9</b>
<b>Table 2 Commonly employed mucoadhesive polymers (adapted from Sandri et. al.49) .....</b>	<b>13</b>
<b>Table 3 Factors affecting mucoadhesion (John et. al. 46 and Shaikh et. al. 48) .....</b>	<b>14</b>
<b>Table 4 Formulation nomenclature.....</b>	<b>24</b>
<b>Table 5 Film compositions (%w/w of solution) .....</b>	<b>24</b>
<b>Table 6 Composition of pH 7.4 Phosphate buffer .....</b>	<b>29</b>
<b>Table 7 Physical characterization of films (Mean±SD, N=3).....</b>	<b>37</b>
<b>Table 8 Tensile (Young's) modulus of commercialy available contact lenses .....</b>	<b>41</b>



## List of Figures

<b>Figure 1 Anatomy of the eye (Adapted from Nigel et. al.5) .....</b>	<b>2</b>
<b>Figure 2 Corneal wound healing process (adapted from Yoon et. al. 13).....</b>	<b>4</b>
<b>Figure 3 Causes of Diabetic Keratopathy .....</b>	<b>6</b>
<b>Figure 4 A schematic of current treatment options for diabetic keratopathy .....</b>	<b>15</b>
<b>Figure 5 Structure of Rebamipide.....</b>	<b>18</b>
<b>Figure 6 Preparation of micropatterned films from PDMS molds .....</b>	<b>22</b>
<b>Figure 7 Nylon mesh well inserts with films .....</b>	<b>28</b>
<b>Figure 8 Texture analyzer setup for mucoadhesion .....</b>	<b>32</b>
<b>Figure 9 Ex-vivo retention time of ocular film .....</b>	<b>34</b>
<b>Figure 10 Light microscopy images of micropatterned films .....</b>	<b>37</b>
<b>Figure 11 Tensile testing of film formulations .....</b>	<b>40</b>
<b>Figure 12 Blue resazurin and its reduced form, red resorufin .....</b>	<b>43</b>
<b>Figure 13 Cell viability .....</b>	<b>44</b>
<b>Figure 14 Standard curve of rebamipide.....</b>	<b>45</b>
<b>Figure 15 Release of rebamipide from different formulations (2.8mg/film) .....</b>	<b>47</b>
<b>Figure 16 Release of rebamipide from 48%EPO+32%FS30D formulations .....</b>	<b>47</b>
<b>Figure 17 Ex-vivo mucoadhesion on porcine intestinal and ocular tissue.....</b>	<b>50</b>
<b>Figure 18 Mucoadhesion on porcine intestinal tissue .....</b>	<b>51</b>
<b>Figure 19 Mucoadhesion of 48%EPO+32%FS30D on porcine ocular tissues.....</b>	<b>52</b>
<b>Figure 20 Ex-vivo retention study of ocular films on the surface of porcine eye .....</b>	<b>54</b>

## Acknowledgements

I would like to express my deepest gratitude to my academic advisor and mentor Dr. Vinayak Sant for his guidance, motivation and valuable counsel throughout my graduate education. With his support and encouragement, I was able to learn a variety of new techniques and develop essential skills. I would also like to thank Dr. Shilpa Sant for constantly encouraging me to explore and pursue ideas and develop innovative methods.

I am extremely grateful to my friends and fellow lab members Huatian Li, Dr. Catalina Ardila, Dr. Vaishali Aggarwal, Julio Aleman and Oshin Miranda for their constant support and advice. I would like to specially thank my past lab members Mrunal Sakharkar, Urmi Chheda and Dr. Akhil Patel for patiently training and mentoring me throughout my research. I am very thankful to Dr. Prema Iyer, Zoe Vaughn, and the undergraduate interns Ishwarya Karthikeyan, Deeptha Gokul and Smriti Suresh for supporting me and being such great friends.

I would like to thank Dr. Lisa Rohan and her lab for training me and allowing me to use the lab equipment for my studies. I am grateful to Prithvirajan Durairajan for his counsel and training. I also express my heartfelt thanks to Dr. Maggie Folan, Lori Altenbaugh, Dolores Hornick and all the faculty, staff and students at the University of Pittsburgh School of Pharmacy.

I would like to express my deepest gratitude to my parents, brother and grandparents for all their love and support. Finally, I would like to thank my dear friends Mrunmayi, Dilisha, and Divyam for being my pillars of support throughout my graduate journey.

## 1.0 Introduction

Diabetes is a chronic disease which affects the way the body utilizes and metabolizes blood sugar. As reported by the CDC<sup>1</sup>, around 30 million adults in the United States have diabetes and it is the seventh leading cause of death. Diabetes is a serious illness due to the numerous co-morbidities associated with it such as nerve damage, kidney disease, heart disease, and ocular problems, among others. Although treatment can significantly alleviate or slow these manifestations and control blood sugar, there exists no cure for diabetes as of today. One among the numerous organs affected by chronically high blood glucose and its impaired metabolism is the eye.

The ocular complications associated with diabetes include glaucoma, diabetic retinopathy, cataract, diabetic papillopathy and surface abnormalities.<sup>2</sup> Diabetic ocular surface diseases are a cluster of abnormalities occurring on the anterior ocular surface of the eye. Diabetic Keratopathy, first reported by Schultz et. al., is the term used to describe these ocular surface complications.<sup>3</sup> It includes the occurrence of corneal surface erosions and delayed wound healing in the cornea. Around 47-64% of the diabetic patients were reported to have some kind of epithelial lesions on the cornea.<sup>3</sup> The corneal epithelium is an essential barrier to the entry of external pathogens into the eye. A breach of this barrier renders a diabetic patient vulnerable to numerous ocular infections. Further, non-healing ulcerations cause the development of scar tissue and severely impair vision.<sup>4</sup> Therefore, there is an urgent need for a simple and effective treatment method for the prevention of recurrent corneal erosions in diabetic patients.

## 1.1 Anatomy and Physiology of the Ocular Surface

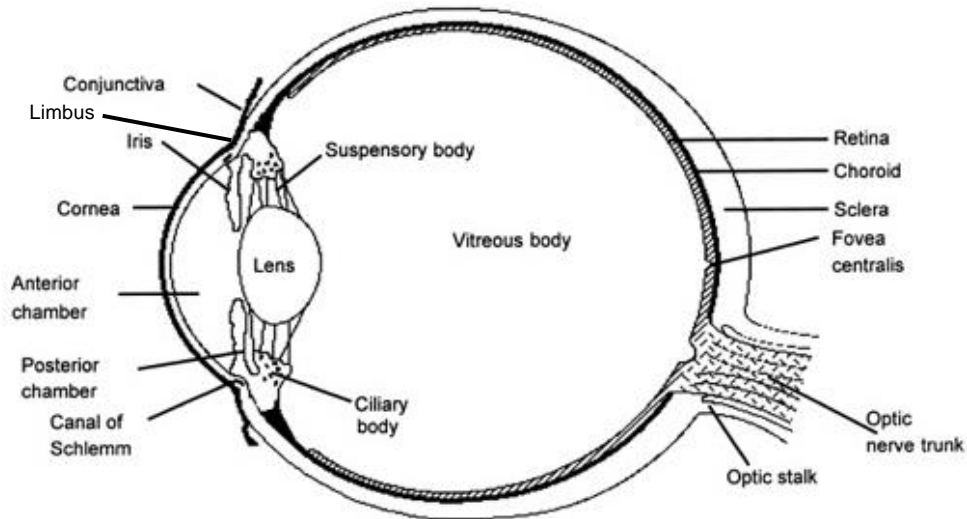


Figure 1 Anatomy of the eye (Adapted from Nigel et. al.<sup>5</sup>)

The anterior segment of the eye consists of the cornea, sclera, conjunctiva, iris, and the pupil. The cornea and the sclera converge at the limbus, which forms a ring around the cornea. The outermost transparent covering of the sclera is a thin layer of mucus-producing cells called the conjunctiva. This layer is continuous with the inside of the superior and inferior palpebrae (eyelids). Covering the cornea is a tri-layered tear film that comprises of a lipid layer, an aqueous layer and a mucin layer that protect the eye from pathogens, dust and the shear caused due to blinking.<sup>6</sup>

The sclera is the white, fibrous, and strong outer covering of the eye comprising of collagen and elastic fibers. The cornea is the transparent, convex, and avascular portion of the eye through which light is transmitted. The average diameter of the cornea is reported to be between 11 and

12mm with a central thickness of around 0.5mm.<sup>7, 8</sup> The cornea consists of the epithelium, the Bowman layer, stroma, the Descemet membrane, and the endothelium. The epithelium consists of 4-6 layers of squamous corneal epithelial cells containing tight junctions that are replaced every 7-10 days.<sup>9</sup> Epithelial inflammation and abrasions in diseases such as diabetic keratopathy cause the loss of tight junctions leading to the vulnerability of the eye towards pathogens. The basal layer of epithelial cells is attached to the Bowman membrane by hemidesmosomes. Hemidesmosomes are cellular junctions that enable cells to tightly adhere to the underlying basement membrane.<sup>10</sup> In diabetic keratopathy, a decrease in the number of hemidesmosomes has been reported.<sup>11</sup> As a result, there is decreased adhesion of the epithelium to the basal lamina. The corneal limbus consists of stem cells that migrate and differentiate to replace lost epithelial cells continually. They also serve as a barrier to prevent the migration of conjunctival cells across the cornea.<sup>12</sup>

## 1.2 Corneal Wound Healing

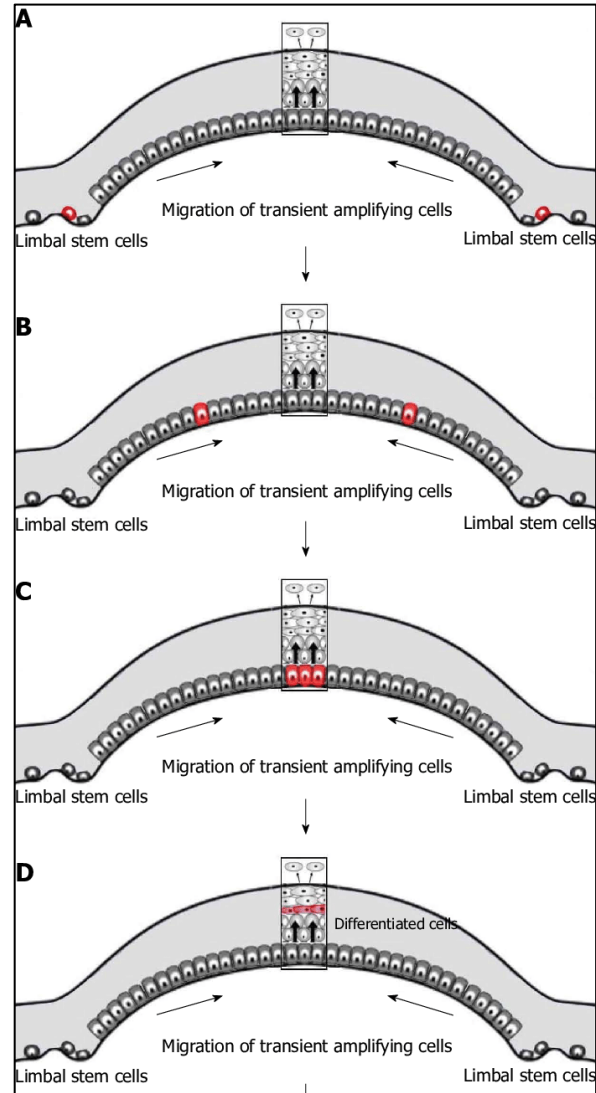


Figure 2 Corneal wound healing process (adapted from Yoon et. al. 13)

An injury to the surface of the cornea initiates a cascade of events that repair and restore the cornea to its normal state. Corneal epithelial wound healing occurs with the help of corneal limbal epithelial cells that are stem cells found in the limbus. Corneal wound healing begins with cell death at the site of injury and is a series of migration, proliferation and differentiation of corneal epithelial cells.<sup>11</sup> Soon after corneal injury, a latent phase ensues in which dead cell are

removed and the cells at the periphery of the wound begin to synthesize structural proteins in preparation for migration.<sup>14 15</sup> This is followed by the migration of epithelial cells from the periphery to cover the wound area and ensure wound closure.<sup>16</sup> The limbal epithelial cells divide and differentiate into corneal epithelial cells to restore cellular mass in the wounded region. Finally, the newly formed cellular layer forms permanent adherent junctions to the basement membrane called hemidesmosomes after the entire wound is closed.<sup>14, 15</sup> Thoft et. al. have hypothesized corneal wound healing to be an  $X+Y=Z$  process in which proliferation of epithelial cells (X) and the centripetal migratory motion of peripheral cells (Y) serves to make up for the loss of epithelium (Z) due to injury.<sup>17</sup>

In diabetic keratopathy, the corneal wound healing process is highly impaired and results in chronic corneal inflammation and erosions. The cornea is one of the most innervated tissues in the body. The corneal nerves are important in maintaining the corneal epithelium and in homeostasis. Chronic diabetes results in the loss in sensitivity of corneal nerves, persistent inflammation, deposition of disruptive advanced glycation end-products (AGE) in the basement membrane and repeated corneal erosions and scarring.<sup>2, 18, 19, 20</sup> AGE deposition is hypothesized to cause basement membrane thickening and improper adhesion of corneal cells to the membrane.<sup>21</sup> Repeated inflammation and the resultant generation of oxidative stress primarily contributes to the non-healing epithelial erosions.<sup>22</sup> Higher levels of reactive oxygen species (ROS) has been reported to decrease the number of tight junctions in the cornea, compromising its barrier function.<sup>23</sup> This severely affects the corneal wound healing process due to a disruption in ocular homeostasis. Recurring erosions that do not heal may finally transition to opaque scar tissue formation, thus impairing vision.

Diabetic individuals also often experience tear film instability and low secretion of mucins on the ocular surface, which contributes to a dry eye-like state.<sup>24</sup> Corneal mucins play an important role in maintaining the lubrication of the corneal surface and preventing cell to cell adhesion between the cornea and the eyelid.<sup>25</sup> They have also been reported to have protective functions by acting as a penetrative barrier to pathogens and external molecules.<sup>25</sup> Overall, the ocular environment in diabetic keratopathy is hostile and this in turn impairs proper healing of corneal erosions and injuries.

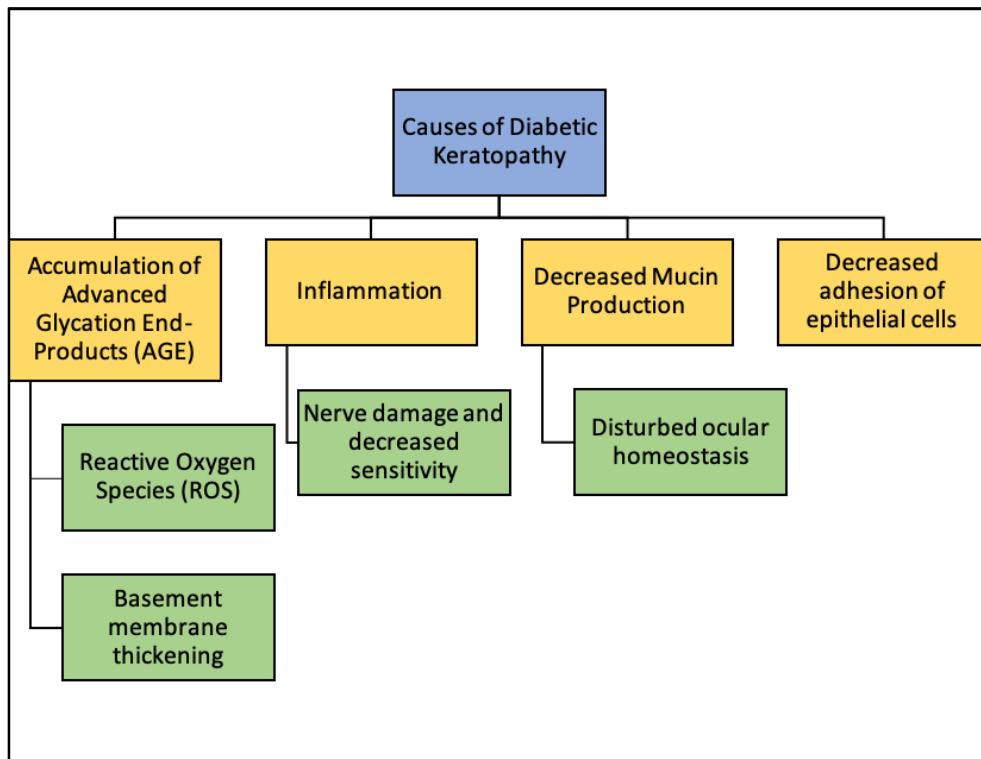


**Figure 3 Causes of Diabetic Keratopathy**



### 1.3 Topical Ocular Drug Delivery

Topical delivery on the ocular surface is the preferred method of administration of drugs for the treatment of ocular surface disorders and form about 90% of all marketed ocular formulations.<sup>26</sup> Drugs are instilled directly into the ocular cavity in the form of drops, gels, inserts, ointments, microneedles, suspensions and other lipid and polymeric systems.<sup>27</sup>

Eyedrops remain the top choice for ocular drug delivery due to the ease of application and patient compliance. However, due to the high clearance rate from the ocular surface, 95% of the administered dose is washed away within a few minutes of instillation. <sup>28</sup> The residence time of an instilled drug on the eye is only about 5 minutes.<sup>29</sup> Current research is therefore focusing on improving the retention of topical dosage forms on the ocular surface (Table 1).

Ophthalmic ointments and gels are designed to improve the release and residence of drug on the ocular surface by increasing the viscosity of the formulation. Ocular ointments are developed with drug incorporated into semi-solid lipids such as lanolin and paraffin. The limitation of ointments include the disturbance of vision due to the lipoidal nature of the vehicle, thus reducing patient acceptability. Further strategies to improve the residence of drug at the target site involve the development of ocular gels. Ophthalmic gelling systems are solutions that utilize a stimulus such as temperature, enzymes or pH to convert to a viscous gel.<sup>30</sup> However, gelling systems also cause a blurring of vision due to their viscosity. Gels may also cause reflexive blinking, resulting in rapid clearance of the formulation from the eye. Colloidal ophthalmic dosage forms include liposomes, micelles, nanoemulsions, nanoparticles and microparticles.<sup>31</sup> Nanoparticles, emulsions and liposomes may be coated or functionalized with mucoadhesive polymers or groups to adhere to the ocular surface. Amniotic membrane (AM) grafts are also widely used as a post-operative healing treatment and for limbal stem cell deficiency (LSCD).<sup>32</sup>

However, AM grafts are unreliable due to possible risks of disease transmission and incompatibility.<sup>33</sup>

Ocular inserts are solid dosage forms that are usually inserted into the conjunctival cul-de-sac. They have high retention potential and the ability to deliver therapeutic doses effectively to the target site. They allow a larger residence time of drug in the ocular cavity as compared to conventional eye drops. One of the earliest sustained release ocular insert system that was widely accepted was the pilocarpine Ocusert® marketed by Alza Corporation. Other examples of successful ocular insert formulations include the Lacrisert® by Bosch and Lomb for the treatment of dry eye, and the ocular therapeutic system (Minidisc).<sup>34</sup> Literature has shown the development of contact lens-based drug delivery.<sup>35, 36, 37</sup> However, this did not translate to commercialization due to variabilities in material properties and poor processability.<sup>38</sup>

Polymeric thin films are types of ocular inserts consisting of a thin, flexible, polymeric drug loaded matrix. A wide variety of film forming polymers can be used in ocular polymeric thin films such as cellulose, cellulose derivatives, polyvinyl alcohol (PVA), polyvinyl pyrrolidone (PVP), poly (lactic-co-glycolic acid) (PLGA), and chitosan, to name a few. The drug release from polymeric films can be modified by incorporating sustained release polymers such as Eudragit ® and high molecular weight cellulose derivatives in the film matrix. Thin films are superior to conventional eyedrops and other ocular dosage forms due to their ability to provide high drug bioavailability at the target site.<sup>39</sup> Mucoadhesive polymeric films are non-invasive and serve as an effective means for delivering and retaining drug for the treatment of ocular surface diseases. Due to their thin and flexible nature, they can be placed in the cul-de-sac with good tolerability. Since ocular films deliver the dose directly to the target site without much loss, this system can allow

reductions in total dose administered. Films also provide greater stability and shelf-life as compared to aqueous formulations.

**Table 1 Methods for improving retention of ocular dosage forms**

<b>Method</b>	<b>Dosage Forms</b>
Enhancing viscosity	Gels, ointments, In-situ gelling systems
Mucoadhesion	Coated nanoparticles, emulsions
Ocular inserts	Thin films, microneedle devices, Ocusert, Lacrisert
Colloidal systems	Liposomes, nanoparticles

## **1.4 Barriers To Ocular Drug Delivery**

### **1.4.1 Tear Film And Tear Turnover**

The first barrier to topical drug delivery in the eye is the tear film and its turnover. The tear film is composed of an outer lipid layer secreted by the Meibomian glands and the inner aqueous layer, which serves as a barrier to drug permeability. The volume of tears in the eye can vary from 7 to 10  $\mu\text{l}$ .<sup>40</sup> The tear turnover rate is about 16% per minute, which increases the wash-off of drug from the surface of the eye.<sup>41</sup>

### **1.4.2 Tight Junctions**

The tight junctions between corneal epithelial cells or the zona occludens (ZO) prevent the permeation of drugs through the paracellular route.<sup>42</sup> The ZO has high paracellular resistance values of about 120  $\Omega\cdot\text{cm}^{-2}$  (human corneal epithelial cells).<sup>43</sup> High tight junction resistance values in other tissues such as the gastric mucosa (2000  $\Omega\cdot\text{cm}^{-2}$ ), colon (300-400  $\Omega\cdot\text{cm}^{-2}$ ), and human bronchia ( $\sim 766 \Omega\cdot\text{cm}^{-2}$ ) have also been reported by studying in-vitro cell models.<sup>44</sup> The tight epithelial junctions also serve as effective barriers to drug permeability by preventing the entry of polar molecules. <sup>45</sup>

### **1.4.3 Nasolacrimal Drainage**

The nasolacrimal duct is responsible for the drainage of pre-corneal fluids away from the ocular space. The maximum volume that can be retained in the eye is about 30 $\mu\text{l}$ , while the rest of

the instilled volume is drained away.<sup>42</sup> Additionally, instillation of topical preparations cause reflexive blinking, which results in faster drainage of the formulation.<sup>41</sup>

These anatomical and physiological barriers pose a challenge to conventional topical ocular drug delivery with respect to dose retention in the eye. Therefore, drug delivery systems with prolonged residence and sustained release in the eye are required to reduce the loss of drugs due to continued drainage from the ocular surface.

## 1.5 Mucoadhesive Drug Delivery

Mucoadhesive drug delivery systems take advantage of the interaction of the anionic mucin glycoprotein chains with various polymeric excipients to form temporary adhesive bonds to improve residence of dosage form. This mechanism is widely explained by the five theories of mucoadhesion:<sup>46, 47, 48</sup>

1. Wetting theory: It describes the spreading of the dosage form over the mucosal surface with a low angle of contact.
2. Diffusion theory: This theory describes the interpenetration of the long mucin chains with the polymer chains to form a strong adhesive bond depending on the depth of penetration.
3. Electronic theory: It involves the exchange of electrons between the anionic mucin glycoproteins and the mucoadhesive polymers.
4. Adsorption theory: It involves weak surface forces such as ionic and Van der Waal's interactions.
5. Fracture theory: It describes the force involved in the separation of the two surfaces after mucoadhesion.

Mucoadhesive drug delivery systems are widely used in a variety of routes including oral, intra-nasal, intra-ocular, buccal, sublingual, vaginal and rectal sites. Mucoadhesive polymer excipients possess the ability to spread and bind to surface mucins, thereby forming strong, temporary adhesive bonds on the mucosal surface and increasing retention time of the dosage forms. Some of the most commonly used mucoadhesive polymers are given in table 2. A combination of wetting and swelling activates these polymers allows them to interact with the mucins, thereby allowing adhesion and retention of the dosage form.

**Table 2 Commonly employed mucoadhesive polymers (adapted from Sandri et. al.<sup>49</sup>)**

<b>Source</b>	<b>Mucoadhesive Polymers</b>
Natural	Chitosan, hyaluronic acid, sodium alginate, gelatin, agarose, gums
Semi-synthetic	Cellulose derivatives: Carboxymethyl cellulose (CMC), Hydroxypropyl methylcellulose (HPMC), Hydroxyethyl cellulose (HEC), Methylcellulose (MC), Sodium carboxymethyl cellulose (Na-CMC)
Synthetic	Poly (acrylic acid)-based polymers, PVA, PVP, Poly (ethylene oxide)

There are various factors governing the formation of mucoadhesive bonds between the dosage form and the mucosal surface. Some of these factors are given in table 3.

**Table 3 Factors affecting mucoadhesion (John et. al. 46 and Shaikh et. al. 48)**

<b>Factor</b>	<b>Effect on Mucoadhesion</b>
Molecular weight	Higher molecular weight polymers interact by entanglement while lower molecular weight polymers interact by interpenetration of chains.
Spatial conformation of chains	Polymer chains with exposed active binding groups show greater mucoadhesion than polymers having coiled chains that shield the binding groups by virtue of their spatial conformation.
Polymer cross-linking	High cross linking prevents hydration of polymer chains and decreases mucoadhesion. Optimum cross-linking is desired to allow swelling and hydration for maximum mucoadhesion
Charge	Mucins have a negative surface charge and are able to interact well with oppositely charged polymers.
Polymer concentration	Increase in polymer concentration results in the increase in the number of chains available for interaction with surface mucins. However, beyond optimum concentration, the coiling of polymer chains results in poor mucoadhesion.
pH	In polymers that have ionizable groups, changes in pH will significantly affect mucoadhesion depending on the pKa of the polymer.



## 1.6 Current Treatment Options For Diabetic Keratopathy

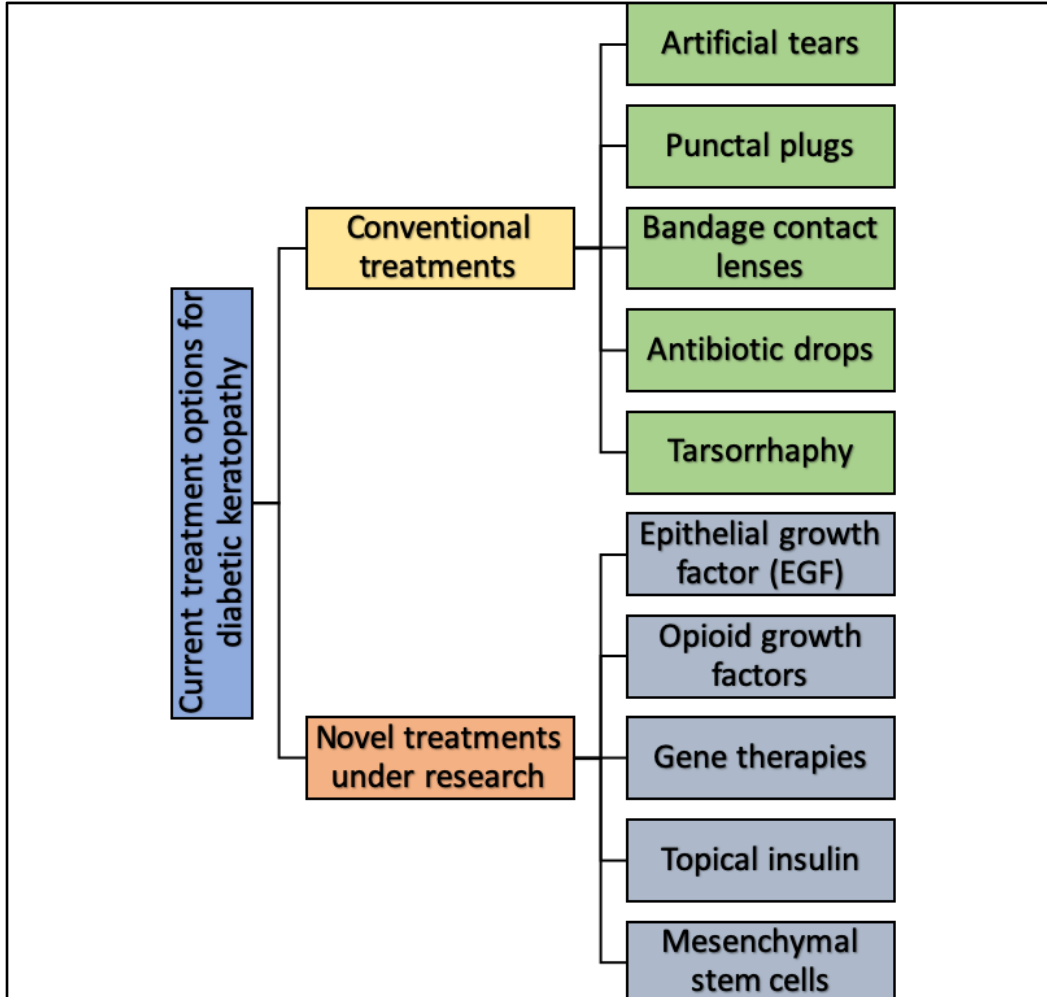


Figure 4 A schematic of current treatment options for diabetic keratopathy

The current treatment for diabetic keratopathy is focused on a symptom-based approach as opposed to cause-based approaches. Artificial tears are majorly prescribed to make up for the damaged tear film and reduced lacrimation by increasing the viscosity of tears and improving tear break-up time.<sup>50, 51</sup> Bandage contact lenses are also used which are protective hydrogel lenses placed over the surface of the cornea to prevent further injury. <sup>52, 53, 54</sup> Antibiotics are administered

for prophylactic purposes to prevent further infection of the compromised cornea by external pathogens. In severe cases, tarsorrhaphy of the eyelids is performed to minimize the exposed surface of the cornea .2, 17, 20 This involves suturing a part or whole of the eyelids together temporarily or permanently to allow the cornea to heal.<sup>55</sup> These treatments, although protective in nature, do not address the underlying cause or assist in wound healing through re-epithelialization of the abraded tissue. To address this problem, research has focused on developing therapeutic growth hormones such as epithelial growth factor (EGF),<sup>56</sup> opioid growth factors,<sup>53</sup> gene therapies,<sup>57</sup> topical insulin,<sup>58</sup> stem-cell treatments,<sup>59, 60</sup> and pharmacological molecules. However, none of these therapies have translated to clinical treatments due to their complexity and variability. Therefore, there is a need for specific treatment that restores the ocular homeostasis and promotes corneal wound healing.

## 1.7 Research Hypothesis

Diabetic keratopathy is a lesser known, potentially sight-threatening, corneal epithelial disease that affects about 47-64% of the diabetic population. Diabetic keratopathy can be associated with a wide array of complications such as increased inflammation, persistent epithelial erosions, non-healing ulcerations, decreased formation of tear fluid, increased generation of reactive oxygen species, and decreased corneal sensitivity. Additionally, diabetic keratopathy is characterized by the loss of both ocular surface and circulatory mucins. Mucins are an important part of the ocular surface. The ocular surface contains both membrane-associated and circulatory mucins. The conjunctiva of the eyelids contains goblet cells that produce the circulating mucins MUC5AC, MUC2 and MUC7.<sup>6</sup> The cornea expresses membrane associated mucins, mainly MUC1, MUC4 and MUC16.<sup>25</sup> Mucins maintain ocular homeostasis and allow normal functioning of ocular tissues. Therefore, the lack of mucins in diabetic keratopathy increasingly contributes to the poor healing of corneal wounds.

Currently employed therapies for the management of diabetic keratopathy are primarily focused on symptomatic treatment, largely involving improved ocular lubrication and prophylaxis against bacterial infections. However, none of the current treatments focus on targeting the cause of corneal inflammation and persistent erosions. Hence, the development of a simple, safe and effective treatment of the underlying cause of diabetic keratopathy is the need of the hour.

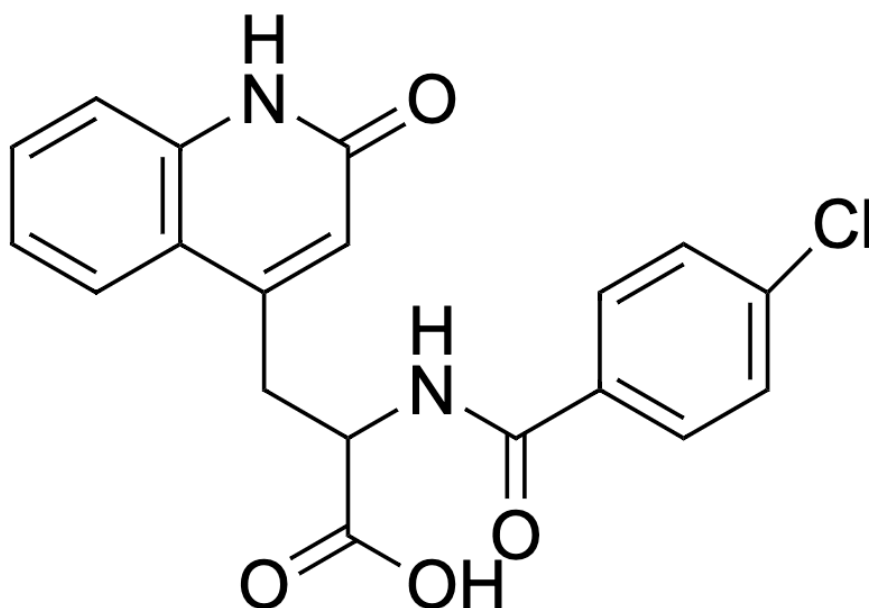


**Figure 5 Structure of Rebamipide**

Rebamipide, a quinolinone drug (Figure 5) manufactured by Otsuka Pharmaceuticals in Japan, has proven to be efficacious in improving the secretion of mucins in both gastric and ocular mucosa.<sup>61, 62</sup> Rebamipide was first introduced as a mucin secretagogue for the treatment of gastric ulcers in *H.pylori* infections and dyspepsia.<sup>63</sup> Further studies on rebamipide's secretagogue activity led to successful clinical trials and the establishment of 2% rebamipide topical ocular suspension as a treatment option for patients with dry eye disease.<sup>61, 64</sup> Rebamipide was shown to improve the stability of the tear film by increasing ocular surface mucin production. <sup>65, 66, 67</sup> It was also proven to improve the secretion of soluble mucins secreted by the conjunctival goblet cells by increasing their numbers.<sup>68</sup> Along with improving mucin secretion, rebamipide also decreased the expression of TNF- $\alpha$  and consequently the expression of interleukin-6 and 8, which resulted in reduced inflammation.<sup>69 70</sup> Further, rebamipide was also shown to reduce ocular inflammation caused due

to the presence of reactive oxygen species.<sup>71</sup> Two case studies reporting the efficacy of rebamipide eye drops on the resolution of persistent corneal epithelial erosions have been published, also demonstrating the efficacy of rebamipide in a diabetic individual with keratopathy.<sup>72, 73</sup> Therefore, rebamipide is a good candidate for the treatment of diabetic keratopathy that targets the underlying causes of corneal epithelial erosions.

The marketed 2% suspension of rebamipide currently has a recommended dosing of 4 drops a day in each eye for 4 weeks for the treatment of dry eye disease.<sup>64</sup> In diabetic keratopathy, the newly formed epithelial tissue is extremely fragile and could possibly be disturbed by the frequent dosing requirements of rebamipide. Additionally, higher dosing frequencies reduce patient convenience and compliance. Therefore, sustained release dosage forms such as mucoadhesive polymeric thin film devices can reduce the dosing frequency of the drug by improving the retention of the drug in the eye. The flexible devices may be placed within the conjunctival cul-de-sac away from the inflamed corneal site to elute small quantities of drug throughout the day. However, as discussed above in diabetic keratopathy, the ocular surface has been reported to suffer from a lack of mucins, which may pose a challenge to the mucoadhesive retention of the thin film device.<sup>74</sup> Therefore, conventional methods of improving mucoadhesion may not be effective.

An interesting study by Arzt et. al. describes the ability of numerous species of insects to stick to smooth surfaces by virtue of the microstructures on their limbs.<sup>75</sup> Studies on insect and gecko adhesion mechanisms elucidated that the microscopic projections or setae on their limbs dictate their ability to adhere to vertical surfaces. Literature indicates that the microscopic setae and their surface roughness increases the surface area in contact with substrates and allows Van der Waals forces to result in strong surface adhesion.<sup>76</sup> Gorb et. al describe a bioinspired tape with

microscopic features that possesses superior adhesive strength and lower contamination potential by virtue of its topography.<sup>77</sup> Hence, the incorporation of micropatterns on polymeric films could potentially serve as an additional retentive mechanism to supplement mucoadhesion in the event of low surface mucin availability. Therefore, in this study, we hypothesize that micropatterned, mucoadhesive films will be retained for long periods on the ocular surface and provide a sustained release of rebamipide for the treatment of diabetic keratopathy.

## **2.0 Materials and Methods**

### **2.1 Materials**

Rebamipide was purchased from TCI America (Portland, OR). EUDRAGIT® FS 30 D and EUDRAGIT® EPO copolymers were kindly gifted by Evonik Industries (Piscataway, NJ). Methocel™ K4M (Hydroxypropylmethyl cellulose K4M) was purchased from Colorcon (West Point, PA) and Natrosol™ 250 (hydroxyethyl cellulose) was obtained from Ashland Global Chemical Company (Wilmington, DE). The plasticizer, polyethylene glycol 400 (PEG 400), was purchased from TCI America (Portland, OR). Polydimethylsiloxane (PDMS) was purchased as the Sylgard 184 Silicone Elastomer Kit from Dow Corning (Midland, MI). Keratinocyte serum free media (KSFM) and Dulbecco's modified Eagle media: Nutrient mixture F-12 (DMEM/F-12) were purchased from Thermo Fisher Scientific (Waltham, MA). Newborn Calf Serum (NCS) was obtained from Sigma-Aldrich (St. Louis, MO). 70µm nylon mesh sterile cell strainers for cytotoxicity studies were purchased from Fisher Scientific (Hampton, NH). Other chemicals and reagents used in formulation preparation were of analytical grade.

## 2.2 Methods

### 2.2.1 Film Preparation

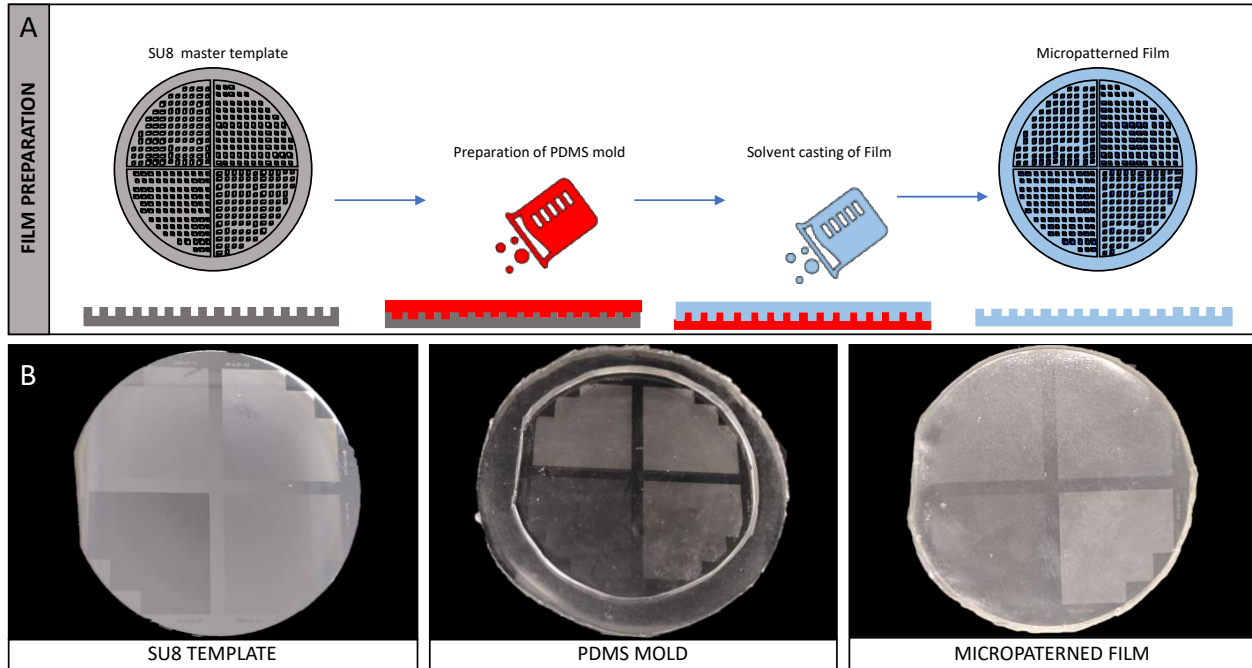


**Figure 6 Preparation of micropatterned films from PDMS molds**

**(A) Soft-lithography preparation of PDMS mold from SU8 template and preparation of micropatterned film by solvent casting. (B) Macroscopic images of SU8 template, PDMS mold and micropatterned film**

Photolithography was used to fabricate silicon wafer master templates having uniform micro-posts of SU-8 photoresist.<sup>78, 79</sup> Soft lithography techniques were then employed to transfer these master patterns on to Polydimethylsiloxane (PDMS) molds using the Sylgard elastomer kit.<sup>80, 81</sup> Micropatterned films with or without rebamipide were prepared by solvent casting of polymeric solutions on the PDMS molds. Briefly, PEG 400 (plasticizer) was weighed and mixed with water to form a uniform solution. Calculated quantities of rebamipide were accurately weighed and



transferred to the solution, forming a fine, milky dispersion. This was followed by sequential addition of polymers with continuous stirring. The polymer dispersion was allowed to stir for 4-5 hours to ensure uniform distribution of rebamipide and Eudragit, and hydration of cellulose. The dispersions were then poured into the PDMS molds and subjected to vacuum cycles to dispel the air incorporated during preparation. The polymeric dispersions were dried in an oven at 70°C for 14-15 hours. The films were gently peeled from the mold and packed in aluminum foil for storage.

### **2.2.2 Formulation Of Polymeric Micropatterned Films**

The polymer solution consisted of a blend of polymers with sustained release properties. The bulk of the solid content of the films consisted of pH sensitive, sustained release poly(meth)acrylate polymers (Eudragits). The two Eudragit polymers chosen were Eudragit FS30D, a methacrylic copolymer and Eudragit EPO, an aminoalkyl methacrylate copolymer. Eudragit FS30D dissolved beyond pH 7 due to its anionic carboxylic acid groups while Eudragit EPO dissolved below pH 5 due to its cationic dimethylaminoethyl groups. Cellulose polymers Natrosol 250L and HPMC K4M were incorporated in smaller amounts as the mucoadhesive component of the films. The total solid content of the films was maintained at 10% w/w of the film solution of which 80% w/w consisted of Eudragits while 20% w/w consisted of cellulose polymers.

Four different formulations were prepared containing varying amounts of Eudragits (Table 5). Since EPO is obtained in powder form, two variants of the EPO-containing formulation were prepared: 80% EPO, which is a fine dispersion of EPO in neutral solution and 80% EPO-A which contains EPO powder dissolved in acidified water along with other components. Therefore, the 80%EPO formulation was a dispersion of EPO in film solution while the 80%EPO-A was a uniform solution of EPO in acidified film solution.

**Table 4 Formulation nomenclature**

<b>Formulation</b>	<b>Sustained Release Polymer</b>
80%FS30D	EUDRAGIT® FS 30 D
80%EPO	EUDRAGIT® EPO
48%EPO+32%FS30D	EUDRAGIT® EPO and FS 30 D
80%EPO-A	EUDRAGIT® EPO

**Table 5 Film compositions (%w/w of solution)**

<b>Film Component</b>	<b>80%FS30D (%w/w)</b>	<b>80%EPO (%w/w)</b>	<b>48%EPO+32 %FS30D (%w/w)</b>	<b>80%EPO-A (%w/w) (Water pH &lt;5)</b>
EUDRAGIT® FS 30 D	26.65	-	10.67	-
EUDRAGIT® EPO	-	8	4.8	8
HPMC K4M	1	1	1	1
HEC 250L	1	1	1	1
PEG 400	4	4	4	4
Distilled Water	67.35	86	78.54	86

## 2.2.3 Physical Characterization Of Films

### 2.2.3.1 Appearance

The micropatterned films were imaged with a Carl Zeiss Primovert inverted microscope (Carl Zeiss Microscopy LLC, WhitePlains, NY) to visualize the patterns on the surface. Images of

different magnifications were captured from the top view and side view to observe pattern shape and height.

### 2.2.3.2 Weight and Thickness

The weight of each film formulation was recorded using a Mettler Toledo DualRange analytical balance (Mettler Toledo, Columbus, OH). Thickness of patterned and unpatterned films was recorded at several points on the film using the Mitutoyo Absolute thickness gauge (Mitutoyo, Japan), the mean and SD were calculated.

### 2.2.4 Tensile Strength

The tensile strength of the micropatterned films was measured using the ADMET MTestQuattro (ADMET, Inc., Norwood, MA) instrument with a 250lbf load cell. The film thickness was measured, and the film was cut into 10 x 20mm<sup>2</sup> rectangular pieces free from surface imperfections and bubbles. The piece was secured between the grips of the tensile tester positioned at a distance of 10mm from each other. The grips were slowly pulled apart at a rate of 10mm/min till the film fractured. The load required to fracture the film was noted as the breaking load. The ultimate tensile strength (UTS) and Young's modulus of elongation was calculated using the following formulae:

$$\text{Ultimate Tensile Strength (UTS)} = \frac{\text{Breaking Load}}{\text{Cross sectional area}}$$

$$\text{Stress} = \frac{\text{Load}}{\text{Cross sectional area}}$$

$$\text{Strain} = \frac{\text{Change in length of film}}{\text{Original length of film}}$$

$$\text{Young's Modulus} = \frac{\text{Stress}}{\text{Strain}}$$

### 2.2.5 Cytotoxicity Of Micropatterned Films On HCLE Cells

Immortalized Human Corneal Limbal Epithelial (HCLE) cells are stem cells in the cornea that differentiate to form the epithelial layer. Immortalized HCLE cells were generously provided to us by Dr. Robert Shanks (Eye & Ear Institute, UPMC, Pittsburgh, PA). The cells were cultured in keratinocyte serum free medium (KSFM) enriched with 25µg/ml bovine pituitary extract (BPE) and 0.2ng/ml epidermal growth factor (EGF). All cultures were maintained at 37°C with 5% CO<sub>2</sub> in a humidified incubator.

Patterned (SQ100D100) films were cut into 12mm inserts containing a 0.25 mg, 0.5mg or 1 mg dose of Rebamipide each. Patterned placebo control films containing no drug were prepared and cut. The films were sewed on to the bottom of nylon mesh well inserts (Figure 7) and then sterilized under UV light for 30 minutes. Solutions of 0.25mg, 0.5mg and 1mg rebamipide were prepared in media as controls. HCLE cells were seeded into 6 well plates at a cell density of 0.75 million cells per well and allowed to adhere overnight. The media was aspirated, and the films were inserted into the well with the patterned side facing the cells. Pure drug in media was added as the reference control. Positive (only cells) and negative (no cells) controls containing no treatments were prepared simultaneously. 4ml of fresh media was added to all the wells and incubated at 37°C with 5% CO<sub>2</sub>. After 24 hours the treatment was removed, and the media was aspirated. 3ml media with 10% v/v resazurin was added to each well and incubated for 1-4 hours to allow metabolism of resazurin. Samples were collected from each well and analyzed for fluorescence with a SpectraMax M5e multi-mode microplate reader (Molecular Devices, San Jose, CA) with absorbance at 560nm and emission at 590nm. Fluorescence of the wells was calculated relative to the positive control to obtain cell viability.

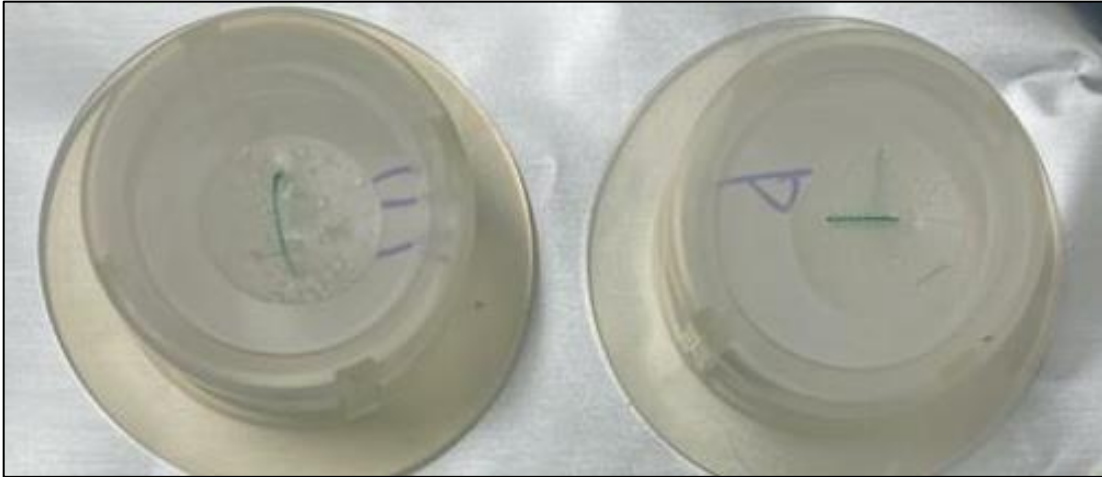


**Figure 7 Nylon mesh well inserts with films**

## 2.2.6 In Vitro Release Of Rebamipide From Films

### 2.2.6.1 Drug Content Of The Films

A stock solution of 1mg/ml of rebamipide was prepared in pH 7.4 phosphate buffer (Table 6). Serial dilutions were performed in buffer to obtain a concentration range of 5-50 $\mu$ g/ml. A full spectrum scan was performed to obtain the maximum absorption wavelength of Rebamipide. A standard curve was plotted using UV Spectrophotometry (NanoDrop OneC; ThermoFisher Scientific, PA) at 327nm.

**Table 6 Composition of pH 7.4 Phosphate buffer**

<b>Ingredient</b>	<b>Quantity Given (g)</b>
Sodium Phosphate monobasic monohydrate	20.214
Sodium phosphate dibasic heptahydrate	3.394
Distilled Water	q.s 1000ml

Three drug-loaded films from each formulation were cut into 10mm or 12mm diameter inserts, weighed and transferred into conical tubes with 10mL of pH 7.4 phosphate buffer. The tubes were ultrasonicated in a Bransonic® bath sonicator (Thomas Scientific, Swedesboro, NJ) to completely dissolve the drug in the buffer. The tubes were centrifuged at 3000 rpm for 5 minutes and the supernatant was collected. The drug content was measured using UV Spectrophotometry (NanoDrop OneC; ThermoFisher Scientific, PA) at 327nm.

### **2.2.6.2 Release Of Rebamipide From Micropatterned Films**

The in-vitro release of rebamipide-loaded films was performed in pH 7.4 phosphate buffer to mimic the pH of tear fluid.<sup>82</sup> The media was placed in a 1.8ml glass vial to simulate the low volumes of the ocular cavity while maintaining good sink conditions. Films were cut into small circular inserts (10 or 12mm diameter) and placed in the vials in 1ml of buffer solution. The vials were then placed in an orbital incubator shaker (Excella E25; New Brunswick Scientific, Edison, NJ) at 37°C and 100 rpm. A 0.4ml of sample was withdrawn from each vial at predetermined intervals and replaced with equal volumes of buffer. A placebo film of each formulation was used as a blank control for measurement. The samples were centrifuged at 1000 rpm and the supernatant was collected. The amount of rebamipide released from the films was analyzed using UV spectrophotometry at 327 nm.



### **2.2.7 Ex-Vivo Mucoadhesion Of Films On Porcine Intestinal And Ocular Tissues**

The mucoadhesive properties of the film formulations were tested using a TA.XT Plus C (Stable microsystems, UK) texture analyzer. The formulations were first screened for their mucoadhesive behavior on the abundantly available porcine intestinal mucosa, followed by porcine ocular tissue sourced from a local slaughterhouse (Thoma Meat Market, Saxonburg, PA). The tissues were transported to the laboratory in a temperature-controlled ice box.

The porcine intestinal tissue was cleaned and cut into pieces of 2cm, placed individually in resealable pouches and stored at -80°C. Prior to the experiment, the intestinal tissue was thawed, cleaned and rinsed with PBS and blotted to remove excess mucins. The tissue was then clamped on to a flat tissue holder at the base of the instrument. The load cell was first calibrated with a weight of 2kg. The film was firmly attached to an 8mm diameter probe with double-sided adhesive tape, which was then affixed to the load cell. The probe was lowered on to the tissue at a speed of 0.5 mm/sec with a force of 10g. A contact time of 60 seconds was maintained to allow the probe to equilibrate on the tissue. The probe was then lifted, and the force required to detach the probe from the mucosal surface was recorded as the peak detachment force (PDF). The work done to detach the two surfaces was recorded as the work of adhesion (WOA).

Enucleated porcine eyes were immersed in PBS containing 1% L-Glutamine, 10% Fetal Bovine Serum and 1% Penicillin-Streptomycin (preservation media) prior to transportation. The eyes were rinsed thoroughly with PBS. The connective tissues were removed from the globes, and the cornea, sclera and eyelids were carefully cut and stored separately in preservation media at 4°C. Within 3 hours of dissection, the ocular tissues were removed from the preservation medium and rinsed with PBS. The experimental procedure for mucoadhesion on ocular tissues remained

the same as that for intestinal tissue. The peak detachment force and work of adhesion was recorded for the films using the sclera, cornea and eyelid tissues.

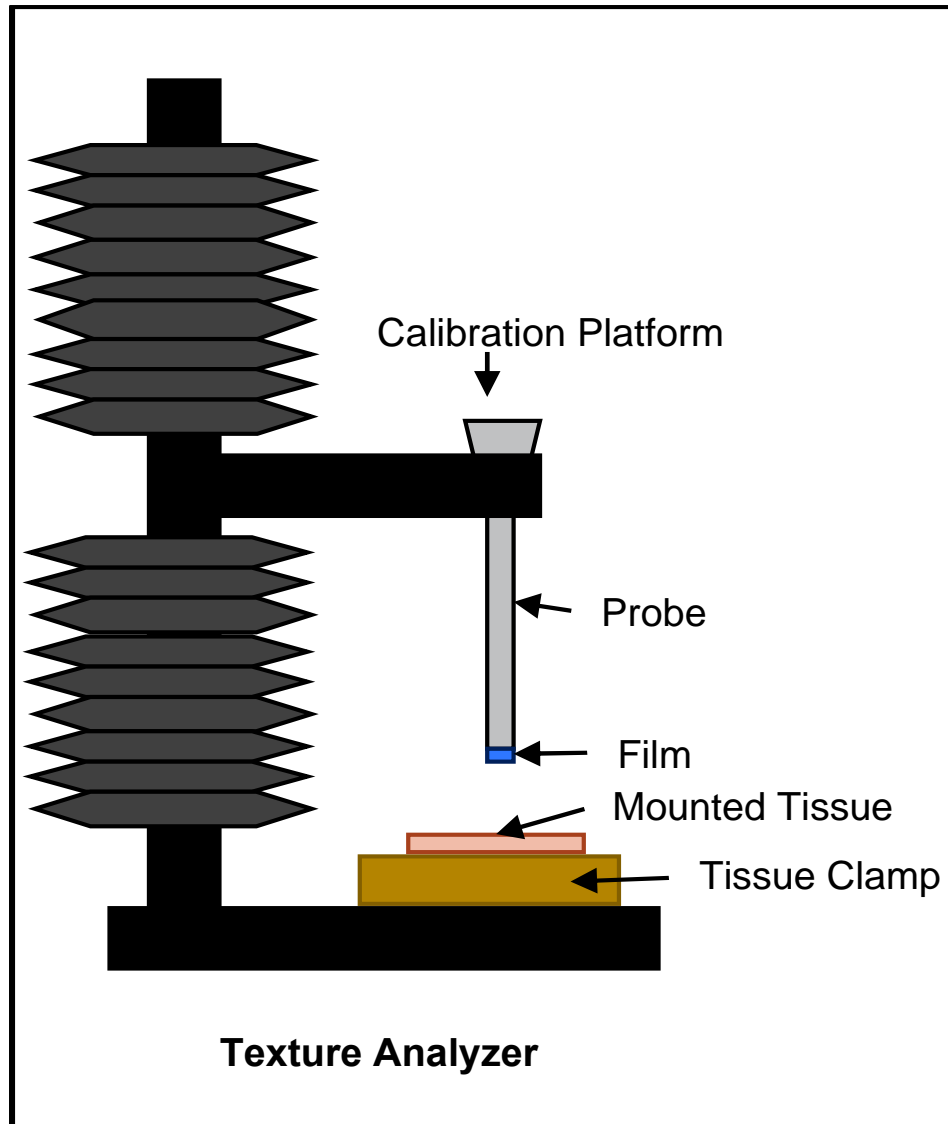
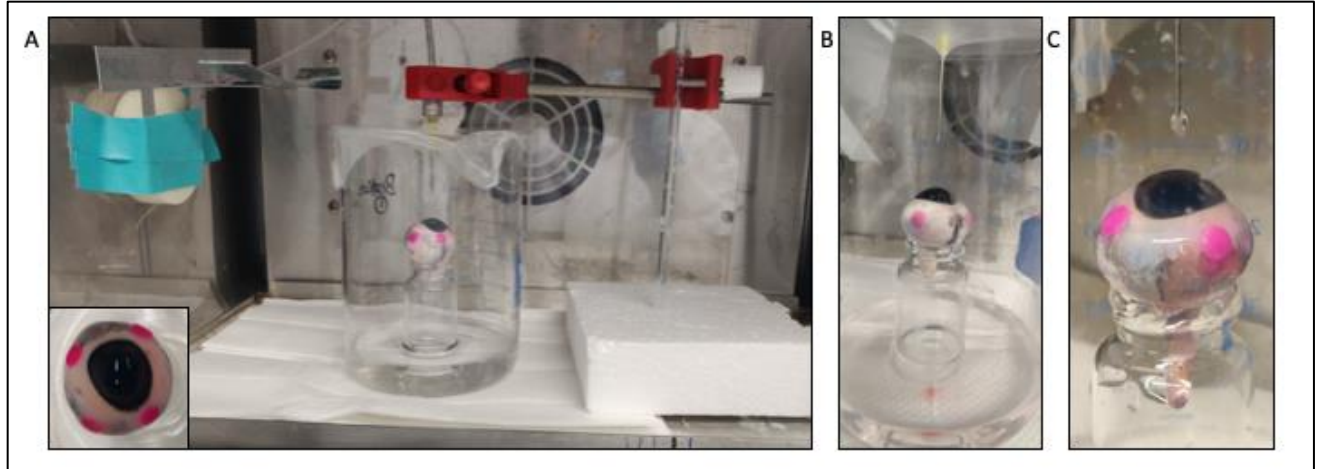


Figure 8 Texture analyzer setup for mucoadhesion

### **2.2.8 Ex-Vivo Ocular Retention Of Micropatterned Films**

The ability of the film to remain adhered when placed on the ocular surface was studied using a newly developed ex-vivo porcine eyeball model. Enucleated porcine eyeballs were cleaned of surrounding connective tissue and placed in preservation media at 4°C. A test setup was constructed as shown in Figure 9 A. A syringe containing PBS maintained at 34°C with the help of a heating jacket was placed in a microfluidic syringe pump. The syringe was connected to a 20G needle by means of tubing. The tube and needle assembly were maintained in place by a clamp within an incubator set at 34°C, the temperature of the ocular surface. The eyeball was rinsed in PBS and held in place inside a beaker containing PBS with the help of a glass vial (Figure 9 B). Two 5mm circular pieces of each SQ100D100 and unpatterned 48%EPO+32%FS30D films were gently placed on the frontal sclera. A pink dye was incorporated into the formulation for visualization. The beaker was covered in parafilm to prevent over-drying of the eyeball and placed under the needle. The pump was turned on and set to deliver 6 drops/min of PBS to the surface of the eye to simulate the flow of tears over the eyeball (Figure 9C). The needle was adjusted such that the drops delivered to the eye were able to evenly spread over the surface. The entire system was maintained undisturbed for a period of 5 hours. The films were observed every 30 minutes for displacement or detachment from the surface. Images of the experimental set up and procedure were recorded with the help of a smartphone camera and documented.



**Figure 9 Ex-vivo retention time of ocular film**

## 3.0 Results and Discussion

### 3.1.1 Film Formulation

Drug bioavailability and clearance are the greatest challenges faced by periocular drug delivery systems. Ophthalmic films are attractive platforms for increasing the residence of drugs on the ocular surface and to sustain drug release. They offer the flexibility for the incorporation of various novel materials such as mucoadhesives and sustained release polymers. Polymeric thin films are prepared by the addition a drug to a film-forming polymeric matrix. The polymers and plasticizers used to fabricate the films in this study are categorized as Generally Recognized as Safe (GRAS) by the FDA. The two major classes of polymers used in the formulation include mucoadhesive cellulose polymers and sustained release Eudragit polymers. Hydroxypropyl methylcellulose (HPMC) K4M is a viscous cellulose polymer used to increase the viscosity of artificial tears and as an excipient in sustained release preparations. It has a viscosity of 4000 MPa.s in a 2% w/v solution in water. Hydroxyethyl cellulose 250L (Natrosol 250L) is a lower viscosity polymer of 75-150 MPa.s in a 5% w/v solution. Cellulose polymers interact with mucin by forming hydrogen bonds between their carboxylic groups and the mucin glycoproteins. Eudragits are methacrylate copolymers that are commonly used sustained release coating polymers for oral drug delivery. Eudragit FS30D is an anionic, carboxylate containing poly(meth)acrylate copolymer dispersion while Eudragit EPO is a cationic, amine containing poly(meth)acrylate polymer powder. These polymers are capable of forming a sustained release matrix that retards the rate of release of drug from the film. Therefore, together the cellulose and eudragit polymers allow sustained release of drug and lend mucoadhesive properties to the film.

### **3.1.2 Polymeric Films Form Good Three-Dimensional Patterns of High Fidelity**

On macroscopic visual inspection, the micropatterned films appeared smooth, uniform, flexible and translucent. Light microscopy images of the micropatterned films clearly show the formation of distinct, 3 dimensional patterns. Figure 10A, 10B and 10C show the formation of the uniform, cuboidal micropatterns at different magnifications. Images of the transverse section of these films confirm the 100-micron height of the 3D pattern projections (Figure 10D and 10E). The patterns were named according to their shape, pattern size and distance between two patterns. As an example, square micropatterns of 100 microns with an inter-pattern distance of 100 microns were named SQ100D100 (Figure 10F). The average weight and thickness of these films is given in Table 7. The thickness of micropatterned films was observed to be around 0.3mm, which is comparable to commercially available formulations such as the Ocusert™ (0.25-0.4mm)<sup>83</sup> and the Lacrisert™ (1.7mm diameter). It was observed that placebo 80%FS30D films had good flexibility and visual appeal while its drug loaded counterpart showed considerable opacity. All the other formulations remained translucent upon loading with rebamipide.

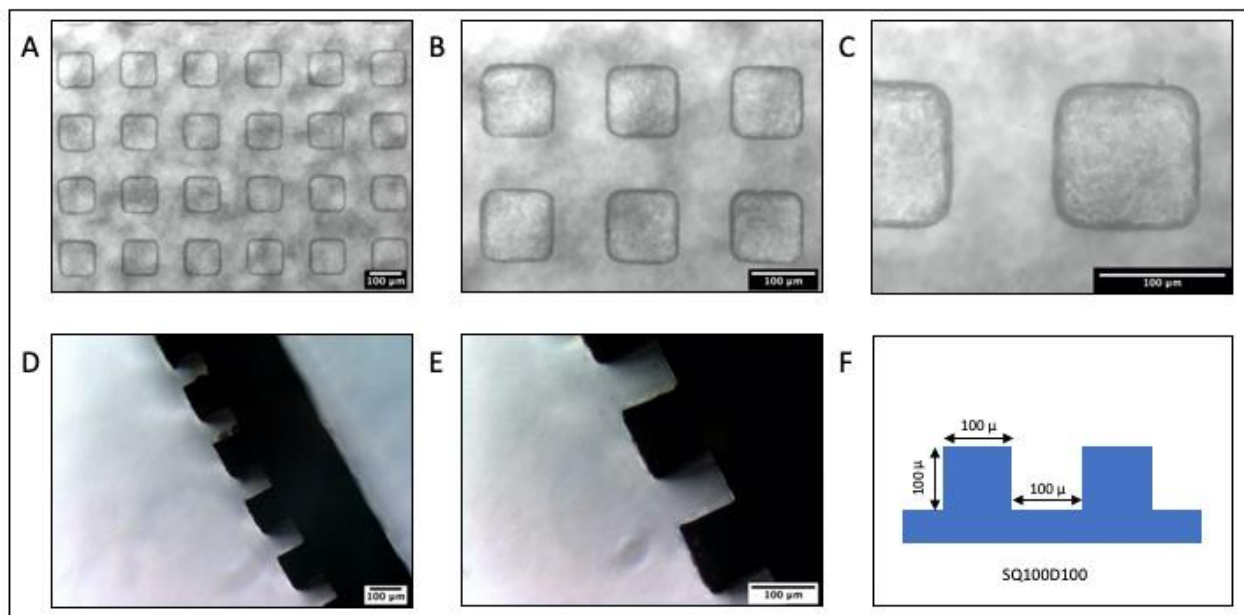


**Figure 10 Light microscopy images of micropatterned films**

**Surface view of SQ100D100 patterns at (A) 10X, (B) 20X and (C) 40X magnifications. Transverse section of the film at (D) 10X and (E)20X showing the height of the patterns. (F) Schematic depicting the pattern dimensions and nomenclature.**

**Table 7 Physical characterization of films (Mean±SD, N=3)**

<b>FORMULATION</b>	<b>WEIGHT OF WHOLE FILM (g)</b>	<b>THICKNESS (mm)</b>
80%FS30D	2.604±0.249	0.305±0.008
80%EPO	2.815±0.148	0.327±0.014
48%EPO+32%FS30D	2.961±0.042	0.317±0.015
80%EPO-A	2.898±0.133	0.315±0.008

### 3.1.3 Micropatterned Polymeric Films Show Good Mechanical Properties

The ultimate tensile strength (UTS) of a film measures the maximum load that the film can withstand before it breaks.<sup>84</sup> The Young's modulus of the film measures its stiffness or ability to withstand stretching due to the application of external load.<sup>85</sup> Higher values of UTS and lower values of Young's modulus indicate that the film can withstand high loads and is an elastic solid. Ocular inserts must be able to withstand the shear stress in the ocular cavity due to blinking. The films must also be easy to handle during the manufacturing process and must be able to withstand peeling from the mold and cutting.

As observed in Figure 11, the 80% FS30D formulation seems to have the lowest Young's modulus values as compared to the other formulations, while the 80% EPO and 80% EPO-A formulations have the largest values. The composite formulation 48%EPO+32%FS30D has intermediate values of Young's modulus, which correlates well with the two extreme formulations. According to literature, polymers with lower values of Young's modulus are classified as elastomeric polymers and possess high flexibility and elasticity.<sup>86</sup> It can be inferred that Eudragit FS30D shows more elastomeric properties as compared to Eudragit EPO. Additionally, the values for Young's modulus of films (~0.02 – 0.3 MPa) are comparable to those obtained from commercially and historically available hydrogel contact lenses (0.1 – 0.8 MPa), as described in Table 8.<sup>87</sup>

UTS follows a reverse trend as compared to Young's modulus, with 80%FS30D having the highest values. As expected, the UTS values of the composite 48%EPO+32%FS30D formulation lie between the two extremes. Typically, the UTS of polymers greatly depends on their molecular weight. Higher molecular weight polymers possess structural entanglements which significantly improves their strength as compared to loose-chained, light polymers.<sup>88</sup> Indeed, it



can be observed that the molecular weight of Eudragit FS30D (~280,000 g/mol) is much greater than that of Eudragit EPO (~47,000 g/mol), which correlates well with this theory.

It can also be observed from the figure that unpatterned films have significantly higher Young's modulus and UTS values as compared to their corresponding patterned films. This is reflected in the observation that in the microscopic fracture characteristics of the film, patterned films indeed fracture in the plain area between the patterns (Figure 11B and 11C) suggesting that the area between patterns is more prone to fracture due to decreased thickness. It may thus be inferred that the unpatterned films have greater potential of withstanding higher loads of extension as compared to patterned films.

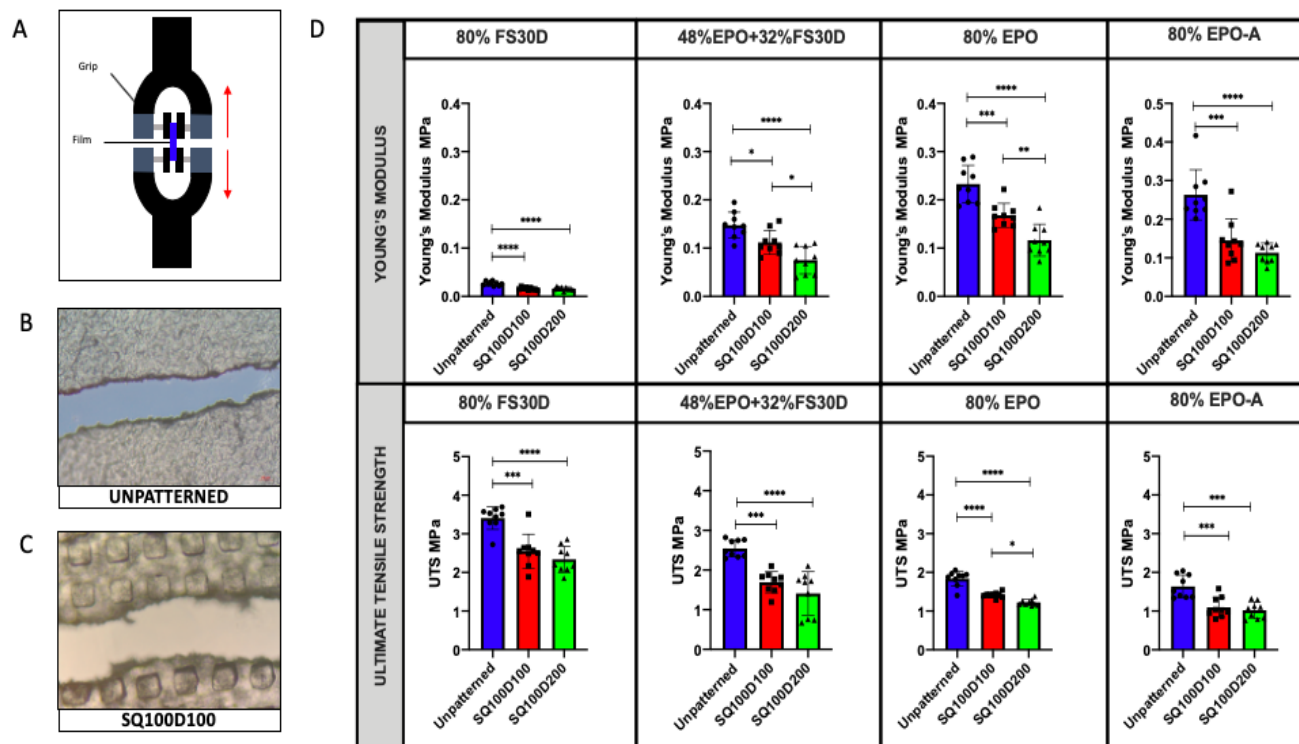


**Figure 11 Tensile testing of film formulations**

A schematic of the mechanical testing setup; (B) and (C) Microscopic images of fracture site in unpatterned and micropatterned films; (D) Measurement of Young's modulus and ultimate tensile strength of unpatterned films, SQ100D100 films and SQ100D200 films by the ADMET MTest Quattro. Data presented as mean  $\pm$  standard deviation for 9 replicates in each group. \*  $p < 0.5$ , One-way ANOVA with Tukey's post hoc test

**Table 8 Tensile (Young's) modulus of commercially available contact lenses**

(adapted from Bhamra et. al.)<sup>87</sup>

<b>Brand Name</b>	<b>Manufacturer</b>	<b>Young's Modulus (MPa)</b>
Cibasoft	Ciba Vision	0.8
SeeQuence	Bausch & Lomb	0.6
Surevue	J&J Healthcare	0.3
B & L Softlens	Bausch & Lomb	0.2
Medalist 66	Bausch & Lomb	0.1

### **3.1.4 Eudragit Containing Micropatterned Films Are Non-Toxic To The Regenerating Corneal Limbal Epithelial Cells**

Human corneal limbal epithelial cells (HCLE) are stem cells of the corneal epithelium that reside at the junction between the cornea and the conjunctiva, known as the corneoscleral limbus. HCLE cells play a major role in epithelial regeneration after corneal injury and thus are the most important players of corneal wound healing.<sup>89</sup> In the event of corneal injury and abrasion, HCLE cells from the limbal niche migrate towards the wound and differentiate to form renewed corneal epithelium.<sup>53, 54</sup> In diabetic keratopathy, the persistent inflammation, recurrent erosions and poor anchorage of basal epithelial cells to the cell membrane results in the loss of equilibrium in the X+Y=Z process of wound healing. Rebamipide, being a scavenger of inflammatory reactive oxygen species and a mucin secretagogue, has been known to significantly improve ocular homeostasis.<sup>73</sup> The main objective of this study was to determine the effect of film formulations and rebamipide on the viability of HCLE cells using the AlamarBlue cell viability assay.

AlamarBlue or resazurin is a redox dye that allows the indirect quantification of cell viability through cellular proliferation and metabolism. <sup>90</sup> The dye is non-toxic, cell-permeable and water soluble. On reduction of resazurin by cellular metabolism, the dye changes to a fluorescent red molecule, resorufin (Figure 12).<sup>91</sup> Fluorescence quantification can be performed at excitation and emission wavelengths of 560nm and 590nm respectively to indirectly obtain viable cell numbers through metabolic activity.

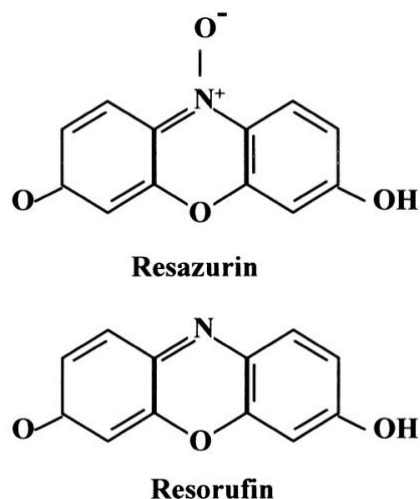


**Figure 12 Blue resazurin and its reduced form, red resorufin**

Exposure of HCLE cells to placebo films of 80%FS30D for 24 hours resulted in around 39% viability. FS30D is soluble above pH 7 and thus results in the dissolution of almost the entire film on incubation in media. Interestingly, 80%FS30D also led to loss in inter-cellular tight junctions of the cells. Exposure to the 80%EPO and 80%EPO-A resulted in even lower viability values of about 4-8%. On microscopic evaluation, a large volume of particulate matter can be observed in the well with a loss in cell junctions. EPO being insoluble below pH 5, precipitates out as particles from the surface of the film due to its high concentration in the formulation. On the other hand, exposure of cells to placebo films of 48%EPO+32%FS30D resulted in a very high viability of about 95% as compared to untreated control (Figure 13 A).

Rebamipide is marketed by Otsuka Pharmaceuticals for the treatment of dry eye as a 2% suspension and has a recommended dose of 4 drops a day.<sup>64</sup> A drug loading of 4mg corresponds to the daily dose of rebamipide in a single eye. However, only about 5% instilled formulations are retained on the target site in the eye.<sup>92</sup> It can thus be crudely inferred that the total bioavailable dose of rebamipide in a day to the eye is only around 0.2mg. Research shows that rebamipide

produces a significant increase in membrane associated mucin secretion in concentrations as low as 10 $\mu$ M in human corneal epithelial cells in vitro.<sup>67, 93</sup> Therefore, the least toxic 48%EPO+32%FS30D composition was formulated into films containing 0.25mg, 0.5mg and 1mg rebamipide. Further testing with these drug-loaded 48%EPO+32%FS30D films resulted in the gradual increase of cytotoxicity with increasing drug loading (Figure 13 B). However, the viability values were comparable to those of HCLE cells when exposed to the same concentrations of pure rebamipide in media. Therefore, it can be inferred that 48%EPO+32%FS30D films containing rebamipide are non-toxic to HCLE cells.

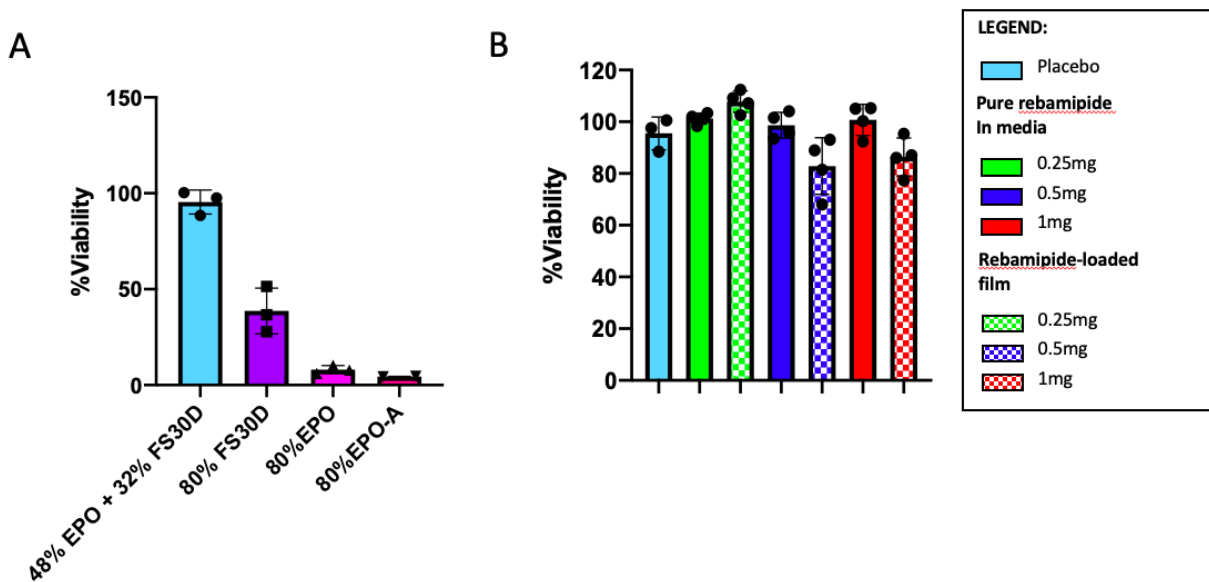


**Figure 13 Cell viability**

**(A)** %Viability of HCLE cells after exposure to placebo films of different compositions

**(B)** %Viability of HCLE cells when exposed to pure drug and drug-loaded films of 48%EPO+32%FS30D

when compared to placebo. Data presented as mean  $\pm$  standard deviation for n= 3 to 4 in each group.

### 3.1.5 Micropatterned Polymeric Films Show A Sustained Release Of Rebamipide Over 24 Hours

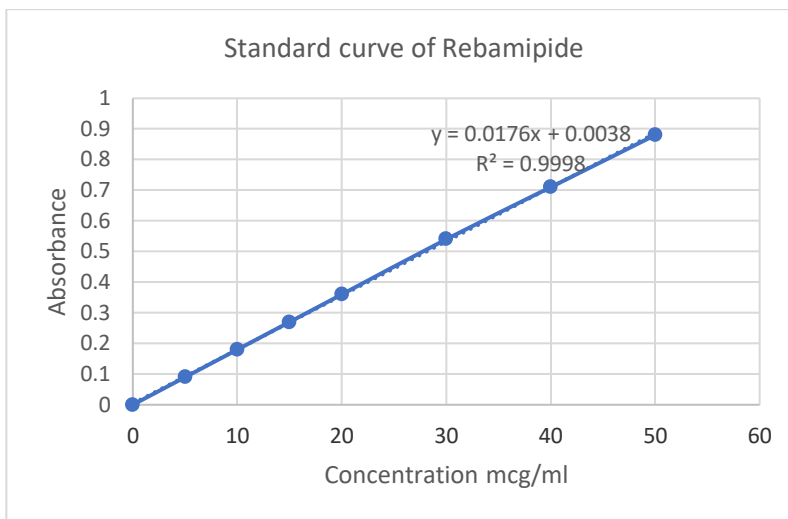


**Figure 14 Standard curve of rebamipide**

Eudragit EPO and Eudragit FS30D serve as release rate modifiers in the micropatterned film formulations. Eudragit EPO remains unionized in the release buffer of pH 7.4 and does not dissolve, thus serving as a sustained release polymer. Eudragit FS30D swells and forms a permeable matrix at pH 7.4 that dissolves with time. In-vitro drug release for rebamipide from the films was performed to determine the sustained release property of the films. Firstly, the standard curve of rebamipide was prepared within the range of  $5\mu\text{g/ml}$  to  $50\mu\text{g/ml}$  and was found to be consistently reproducible (Figure 14). Further, to optimize the protocol and assess the release profiles of the different compositions, 10mm circular samples theoretically containing 2.8mg drug were cut from the films and placed in 1ml of pH 7.4 phosphate buffer. The release profile for rebamipide from the four different formulations is shown in Figure 15. Films containing 80% FS30D dissolved within 3 hours and provided a burst release of drug due to the property of FS30D

to dissolve above pH 7. The 48%EPO+32%FS30D formulation resulted in insoluble films that released approximately 90% of rebamipide in 24 hours. The formulations containing 80% EPO showed a good sustained release of drug with about 60% release in 24 hours. Eudragit EPO does not dissolve at ocular pH (7.4), allowing the slower release of drug from the matrix. Thus, increasing the percentage of EPO polymer in the films improves the release profile of rebamipide. However, according to the cytotoxicity studies, the 80% FS30D, 80%EPO and the 80%EPO-A formulations show high levels of cell death. Therefore, the 48%EPO+32%FS30D formulation is the optimum composition for a non-toxic film with a good release profile.

Further, films of 12mm diameter (approximately 1sq. cm) containing 0.25mg, 0.5mg and 1mg doses of rebamipide in the 48%EPO+32%FS30D were analyzed for drug release (Figure 16). It was observed that the formulations containing 0.25mg and 0.5mg drug released about 80% of drug within the first 3 hours. However, the films containing 1mg of Rebamipide released upto 80% of the drug only after 12 hours. This profile was similar to that observed with higher drug loading of 2.8mg/insert. Current research indicates that the daily dose of rebamipide suspension for the treatment of dry eyes is 1 drop in each eye, 4 times a day.<sup>61</sup> This ophthalmic film formulation of 1mg of Rebamipde per insert allows a sustained release of drug from the matrix, enabling the reduction of dosing frequency and may help improve patient compliance.



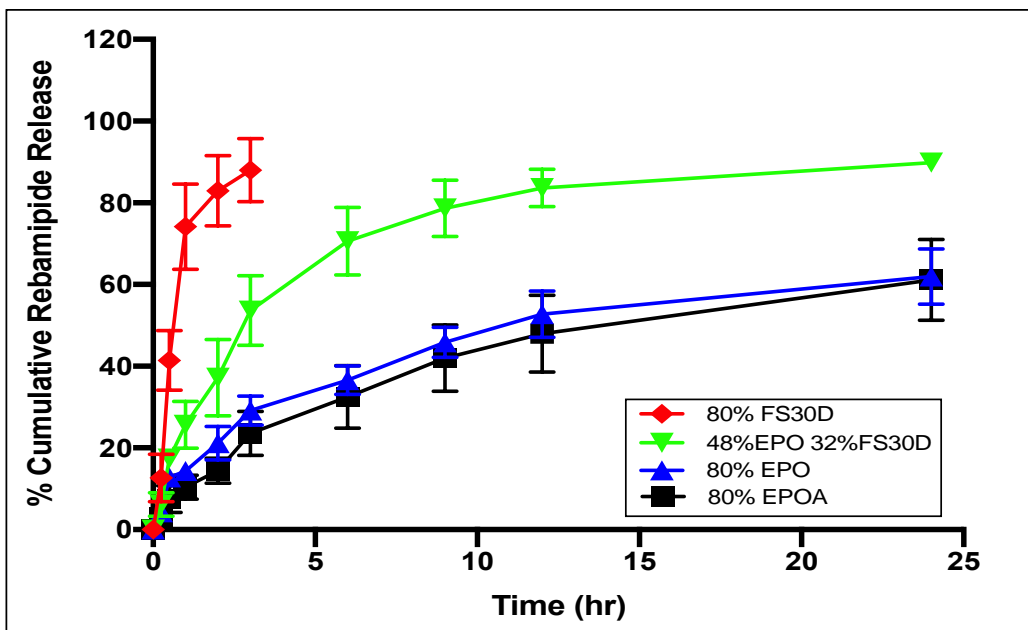


Figure 15 Release of rebamipide from different formulations (2.8mg/film)

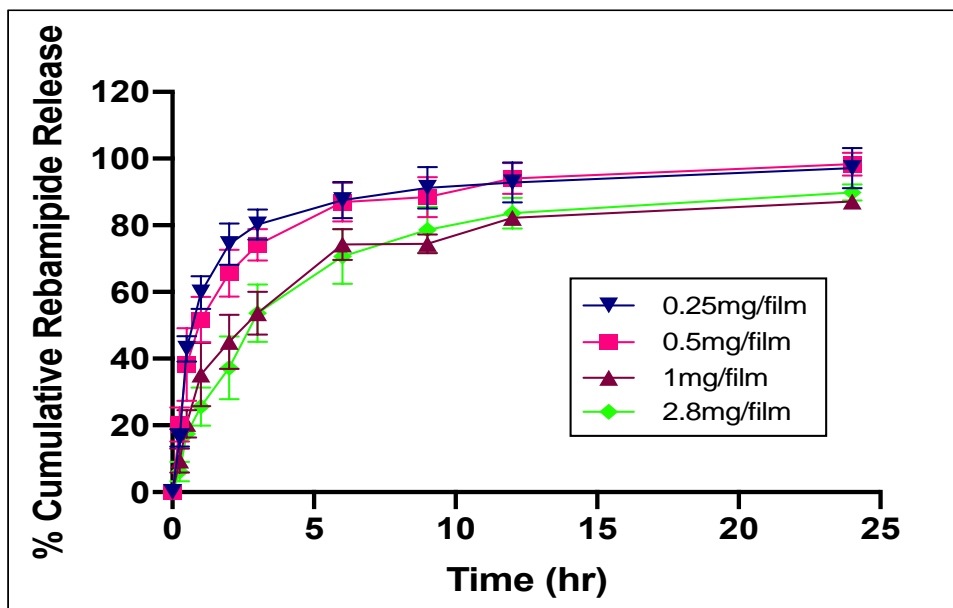


Figure 16 Release of rebamipide from 48%EPO+32%FS30D formulations containing different loadings of rebamipide.

### **3.1.6 Micropatterned Films Possess Higher Mucoadhesion To Ocular Tissues As Compared To Unpatterned Films**

Mucoadhesion is the adhesive force between a material and a mucosal membrane.<sup>94</sup> Mucoadhesive drug delivery systems take advantage of the adhesive interactions between bio-membranes and polymer excipients to increase the retention time of the dosage form.<sup>47</sup> Retention on the ocular surface is paramount for the sustained release of the drug from the film. Peak detachment force is a measure of the force required to detach a material from a mucosal surface while work of adhesion measures the work done to separate the two surfaces. Literature indicates that mucoadhesion is a means to prevent the movement of the dosage form in the eye, thereby preventing further inflammation.<sup>48</sup>

As seen in Figure 18 for porcine intestinal tissue, only 80%FS30D showed a significant difference between work of adhesion for unpatterned and patterned films of SQ100D100 and SQ100D200 patterns. The peak detachment force for the same formulation, although not significant, showed a similar trend. However, the porcine intestinal mucosal tissue contains an abundance of mucins as compared to the ocular surface. This could result in the masking of the effect of patterns on tissue adhesion. Additionally, the folds present on the surface of intestinal mucosa resulted in high tissue-to-tissue variability. In an attempt to obtain more relevant results, the films were then tested for mucoadhesion on porcine ocular tissue. Owing to difficulty in processing and short stability of porcine ocular tissues, only formulations with promising release profiles (80%EPO-A) and cytotoxicity values (48%EPO+32%FS30D) were tested.

The 48%EPO+32%FS30D formulation showed a significant difference in the work of adhesion on the cornea with the SQ100D200 patterns (Figure 19). There were no significant differences between patterned and unpatterned films on the sclera and eyelid. However, similar

trends were observed between 80%EPO-A and 48%EPO+32%FS30D on the sclera, with the SQ100D100 and SQ100D200 patterns. A simple explanation for this behavior could be that the more crowded 100D100 patterns are able to hold on tighter to the surface mucins as compared to the more spaced-out 100D200 patterns. Additionally, the 100D100 patterns have a higher surface area for greater contact with the tissue as compared to both the 100D200 and the unpatterned films. Therefore, we can infer that micropatterns enhance the mucoadhesion and retention of the ophthalmic films on the ocular surface.

In diabetic keratopathy, placement of the films on the sensitive cornea would result in further injury, inflammation and impairment of vision. Patterned films show a good mucoadhesion on the sclera as seen in Figure 19. The ocular inserts therefore may be placed on the sclera within the conjunctival cul-de-sac, akin to other marketed ocular inserts such as pilocarpine Ocuserts<sup>®</sup><sub>95</sub> and cellulose-based lubricant inserts or Lacrisert<sup>®</sup>.<sup>96</sup> This prevents the interaction of the device with the injured cornea. The improved mucoadhesive properties of micropatterned films will enable these films to adhere to the ocular surface after placement and prevent it from dislodging.

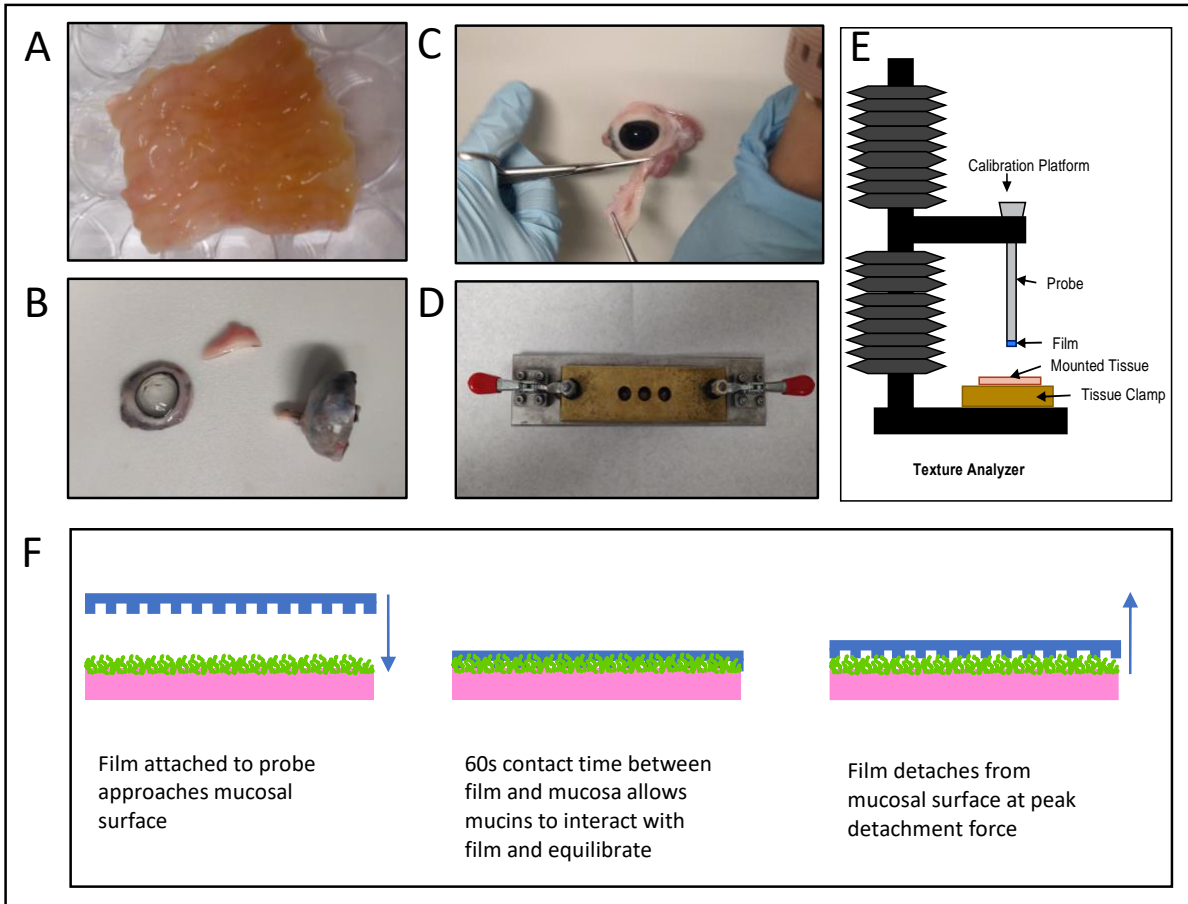


**Figure 17 Ex-vivo mucoadhesion on porcine intestinal and ocular tissue**

**(A) Porcine intestinal tissue; (B) Porcine cornea, eyelid and sclera (left to right); (C) Removal of excess connective tissue from the surface of porcine eye; (D) Tissue clamp; (E) Texture analyzer mucoadhesion set-up**

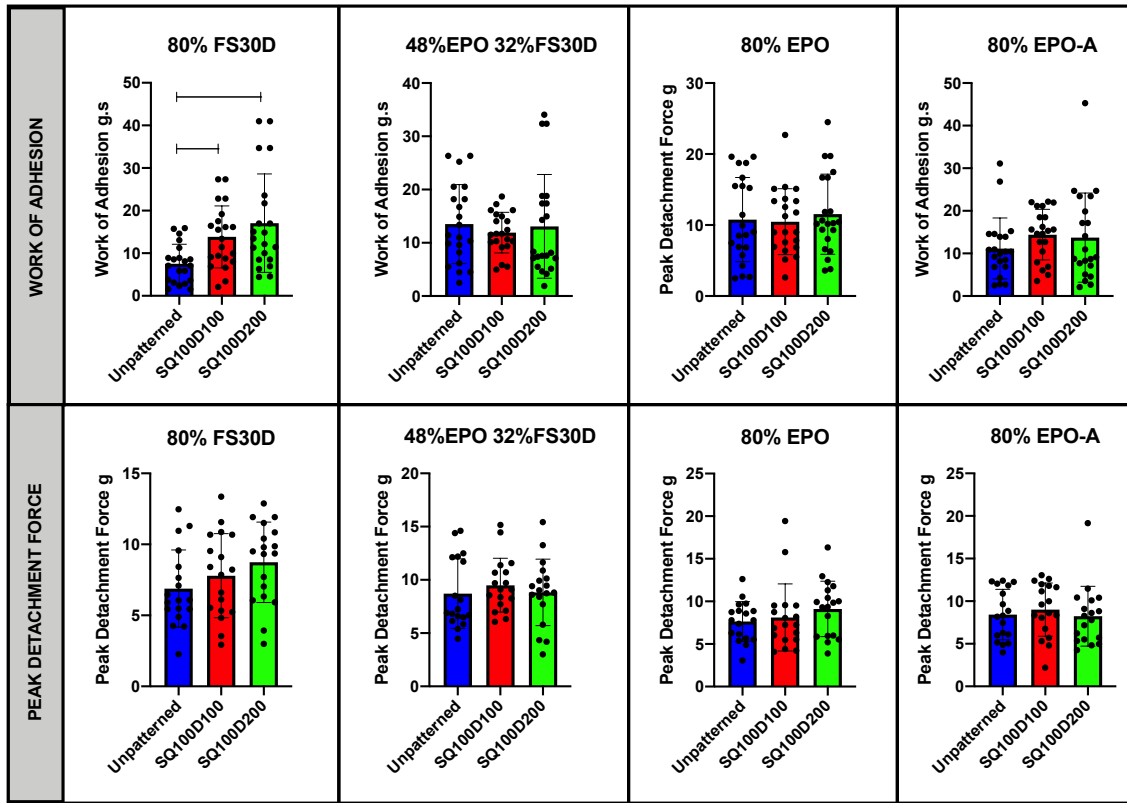
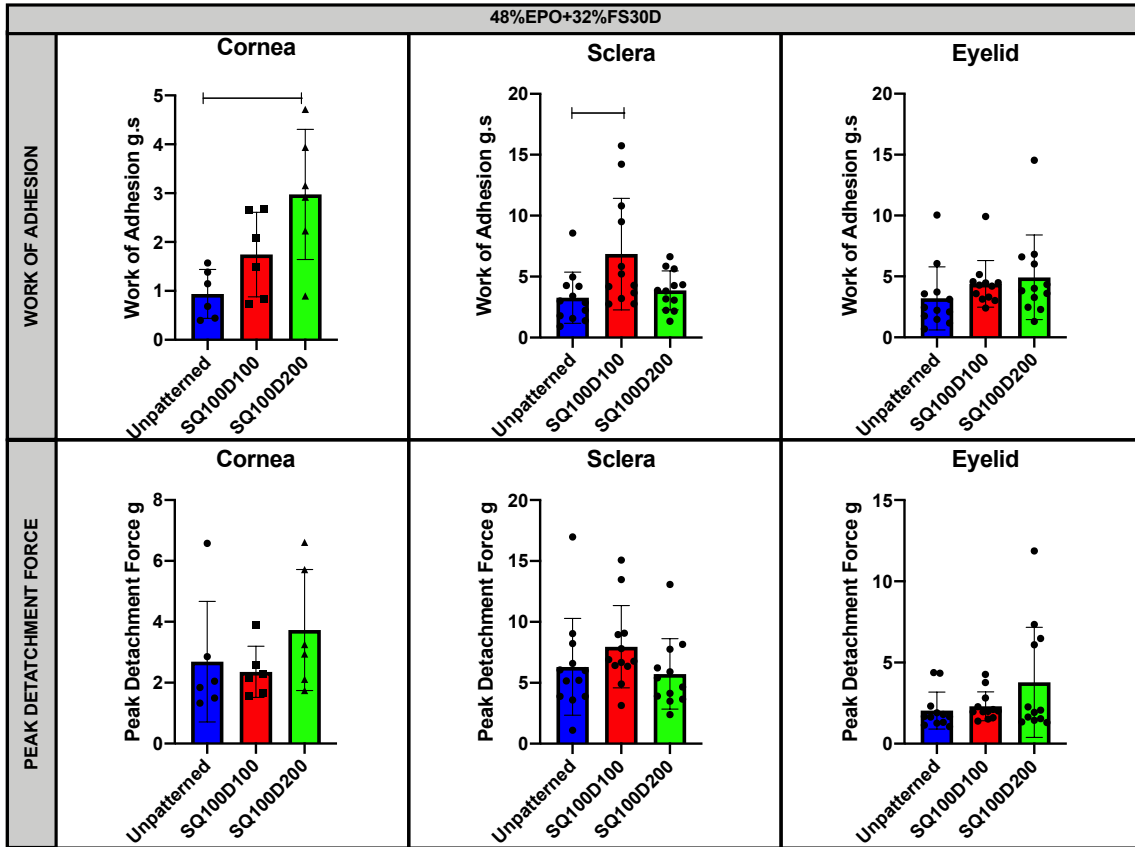


Figure 18 Mucoadhesion on porcine intestinal tissue

Data presented as mean  $\pm$  standard deviation for 18 replicates in each group. \*  $p < 0.5$ , One-way ANOVA with Tukey's post hoc test



**Figure 19 Mucoadhesion of 48%EPO+32%FS30D on porcine ocular tissues**

Data presented as mean  $\pm$  standard deviation for 6 to 9 replicates in each group. \*  $p < 0.5$ , One-way ANOVA

with Tukey's post hoc test

### **3.1.7 48%EPO+32%FS30D Films Are Retained On The Sclera For More Than 5 Hours In The Ex-Vivo Eyeball Model**

The ocular surface has a tear volume of about 7-10 $\mu$ l with a tear turnover rate of 1.2  $\mu$ l per minute.<sup>97</sup> In an effort to understand the behavior of ocular inserts in the presence of lacrimation, an ex-vivo model was developed using porcine eyeballs. The inserts were placed on the anterior sclera that possessed the conjunctival membrane (Figure 20). It was observed that both the patterned and unpatterned 48%EPO+32%FS30D films were retained on the anterior sclera for more than 5 hours. There was no observed dislocation due to simulated lacrimation at 6 drops/minute. It was also observed that the inserts turned visibly opaque on hydration. The pink dye incorporated in the formulation slowly leached out of the film, indicating the constant flow of PBS over the insert. An interesting observation in this study was that the ocular films do not lose their integrity on hydration. On manual removal of films from the surface of the eyeball after completion of the test, it was observed that the films detached without breaking or losing structure. Therefore, this implies that the ocular films can be removed intact after usage. However, this model is still preliminary and requires optimization. Further studies involving acceleration of the drop rate and reducing the distance between the two inserts on the eye may provide better insights on the difference in adhesion between patterned and unpatterned films.



**Figure 20 Ex-vivo retention study of ocular films on the surface of porcine eye**



#### 4.0 Conclusions And Future Directions

The current study has successfully demonstrated the formulation of mucoadhesive, micropatterned polymeric films containing rebamipide as a candidate for the treatment of diabetic keratopathy. The utilization of release modifying Eudragit polymers combined with the soluble, viscous matrix-building cellulose polymers HPMC K4M and HEC 250L resulted in a non-bioerodable ocular insert with sustained release properties. Further, the study shows that solvent casting of films on PDMS molds yield robust micropatterns with good fidelity.

Micropatterned films had varying tensile properties depending on the formulation. The 80% FS30D formulation showed very elastic and flexible behavior while the 80% EPO and 80% EPO-A formulations were tough and brittle. The 48%EPO+32%FS30D formulation showed intermediate values of elasticity and toughness due to blended properties of both Eudragits. Patterned films seemed to be less tough as compared to unpatterned films and fractured along the space between the patterns. The load cell used for the tensile studies was 250lbf, which may not be sensitive enough to capture smaller changes in load with time. Therefore, future studies with a more sensitive load cell are required to confirm the tensile behavior of these films more closely.

Cellular viability of HCLE cells when exposed to placebo films of all formulations was found to be greatest in the combination formulation of 48%EPO+32%FS30D. Viability also seemed to decrease with an increase in drug content from 0.25mg to 1mg drug per insert. The formulations containing 80% FS30D and 80%EPO were extremely cytotoxic with almost negligible cell viability due to polymer dissolution and precipitation respectively. Additional cytotoxicity studies with stratified corneal epithelial cells and conjunctival epithelial cells may be

performed in the future to obtain a complete picture of the cellular effect of the thin film formulation on the eye.

We have successfully achieved a sustained release of up to 87% rebamipide in 24 hours, thus reducing dosing frequency of rebamipide. Additionally, we have demonstrated the incorporation of rebamipide, a poorly water-soluble drug, into the polymeric thin film formulation. However, the drug loading efficiency for 0.25mg, 0.5mg and 1mg rebamipide loaded inserts was only about 80% of added drug. Therefore, further studies must focus on dose optimization, improvement in loading efficiency.

Further, we show the differences in mucoadhesive properties of films between different parts of the ocular surface including the cornea, sclera and eyelids. Since the film formulation was designed to be placed on the anterior sclera within the ocular cul-de-sac, it is interesting to observe that SQ100D100 micropatterns seem to have better mucoadhesion as compared to the unpatterned counterpart. In diabetic keratopathy, there is a decrease in goblet cells, circulating mucins and membrane associated mucins on the ocular surface. Here, the micropatterned films having greater mucoadhesion due to their Velcro-like effect could be advantageous in providing additional retention of the dosage form. Additionally, the preliminary ex-vivo ocular study showed that the 48%EPO+32%FS30D films remain attached to the sclera for over 5 hours even under the continuous flow of PBS over the inserts. Future studies in this direction can be focused on the effects of ocular shear force on the ocular inserts caused due to the blinking motion of the eye. Detachment studies supplemented with shear adhesion studies can be used to more completely predict the behavior of these films when placed in the eye.

In conclusion, this research study demonstrates the potential of micropatterned, mucoadhesive films in sustained drug delivery to the ocular surface and reduce the dosing

frequency of rebamipide in diabetic keratopathy. Through the use of rebamipide, we have developed a cause-based therapeutic approach for the treatment of diabetic keratopathy. Additionally, we have developed a novel method of enhancing the mucoadhesion of ocular films by the fabrication of micropatterned surfaces. Further studies are required to assay the functional effect of rebamipide-loaded on the secretion of ocular mucins and to decrease the insert size to one that is closer to commercially accepted products. Finally, due to the hostile nature of the ocular environment in diabetic keratopathy, an additional parameter that remains to be studied is the effect of micropatterned films on ocular inflammation.

## Bibliography

1. Centers for Disease Control and Prevention UDoHaHS. National Diabetes Statistics Report, 2020. (ed<sup>^</sup>(eds) (2020).
2. Sayin N, Kara N, Pekel G. Ocular complications of diabetes mellitus. *World journal of diabetes* **6**, 92-108 (2015).
3. Schultz RO, Van Horn DL, Peters MA, Klewin KM, Schutten WH. Diabetic keratopathy. *Transactions of the American Ophthalmological Society* **79**, 180-199 (1981).
4. Bu Y, *et al.* Experimental modeling of cornea wound healing in diabetes: clinical applications and beyond. *BMJ Open Diabetes Research & Care* **7**, e000779 (2019).
5. Davies NM. Biopharmaceutical Considerations In Topical Ocular Drug Delivery. *Clinical and Experimental Pharmacology and Physiology* **27**, 558-562 (2000).
6. Davidson HJ, Kuonen VJ. The tear film and ocular mucins. *Veterinary Ophthalmology* **7**, 71-77 (2004).
7. Rüfer F, Schröder A, Erb C. White-to-White Corneal Diameter: Normal Values in Healthy Humans Obtained With the Orbscan II Topography System. *Cornea* **24**, 259-261 (2005).
8. DelMonte DW, Kim T. Anatomy and physiology of the cornea. *Journal of Cataract & Refractive Surgery* **37**, 588-598 (2011).
9. Sridhar MS. Anatomy of cornea and ocular surface. *Indian journal of ophthalmology* **66**, 190-194 (2018).
10. Torricelli AAM, Singh V, Santhiago MR, Wilson SE. The corneal epithelial basement membrane: structure, function, and disease. *Investigative Ophthalmology & Visual Science* **54**, 6390-6400 (2013).
11. Ljubimov AV, Saghizadeh M. Progress in corneal wound healing. *Progress in retinal and eye research* **49**, 17-45 (2015).
12. Dua HS, Azuara-Blanco A. Limbal Stem Cells of the Corneal Epithelium. *Survey of Ophthalmology* **44**, 415-425 (2000).
13. Yoon JJ, Ismail S, Sherwin T. Limbal stem cells: Central concepts of corneal epithelial homeostasis. *World journal of stem cells* **6**, 391-403 (2014).

14. Dua HS, Gomes JA, Singh A. Corneal epithelial wound healing. *British Journal of Ophthalmology* **78**, 401 (1994).
15. Agrawal V, Tsai R. Corneal epithelial wound healing. *Indian journal of ophthalmology* **51**, 5-15 (2003).
16. Zagon IS, Sassani JW, McLaughlin PJ. Cellular dynamics of corneal wound re-epithelialization in the rat: I. Fate of ocular surface epithelial cells synthesizing DNA prior to wounding. *Brain Research* **822**, 149-163 (1999).
17. Thoft RA, Friend J. The X, Y, Z hypothesis of corneal epithelial maintenance. *Investigative Ophthalmology & Visual Science* **24**, 1442-1443 (1983).
18. Wang B, *et al.* A comparative study of risk factors for corneal infection in diabetic and non-diabetic patients. *Int J Ophthalmol* **11**, 43-47 (2018).
19. Shih KC, Lam KSL, Tong L. A systematic review on the impact of diabetes mellitus on the ocular surface. *Nutrition & diabetes* **7**, e251-e251 (2017).
20. Abdelkader H, Patel DV, McGhee C, Alany RG. New therapeutic approaches in the treatment of diabetic keratopathy: a review. *Clin Exp Ophthalmol* **39**, 259-270 (2011).
21. Kaji Y. Prevention of diabetic keratopathy. *The British journal of ophthalmology* **89**, 254-255 (2005).
22. Sun H, *et al.* Inhibition of Soluble Epoxide Hydrolase 2 Ameliorates Diabetic Keratopathy and Impaired Wound Healing in Mouse Corneas. *Diabetes* **67**, 1162-1172 (2018).
23. Jiang Q-w, *et al.* Diabetes inhibits corneal epithelial cell migration and tight junction formation in mice and human via increasing ROS and impairing Akt signaling. *Acta Pharmacologica Sinica* **40**, 1205-1211 (2019).
24. Ljubimov AV. Diabetic complications in the cornea. *Vision Res* **139**, 138-152 (2017).
25. Mantelli F, Argüeso P. Functions of ocular surface mucins in health and disease. *Current opinion in allergy and clinical immunology* **8**, 477-483 (2008).
26. Dubald M, Bourgeois S, Andrieu V, Fessi H. Ophthalmic Drug Delivery Systems for Antibiotherapy-A Review. *Pharmaceutics* **10**, 10 (2018).
27. Souza JG, Dias K, Pereira TA, Bernardi DS, Lopez RFV. Topical delivery of ocular therapeutics: carrier systems and physical methods. *Journal of Pharmacy and Pharmacology* **66**, 507-530 (2014).
28. Le Boultais C, Acar L, Zia H, Sado PA, Needham T, Leverge R. Ophthalmic drug delivery systems—Recent advances. *Progress in retinal and eye research* **17**, 33-58 (1998).

29. Ali M, Byrne ME. Challenges and solutions in topical ocular drug-delivery systems. *Expert Review of Clinical Pharmacology* **1**, 145-161 (2008).
30. Kumar S, Haglund BO, Himmelstein KJ. In Situ-Forming Gels for Ophthalmic Drug Delivery. *Journal of Ocular Pharmacology and Therapeutics* **10**, 47-56 (1994).
31. Al-Kinani AA, Zidan G, Elsaid N, Seyfoddin A, Alani AWG, Alany RG. Ophthalmic gels: Past, present and future. *Advanced Drug Delivery Reviews* **126**, 113-126 (2018).
32. Wright B, Mi S, Connon CJ. Towards the use of hydrogels in the treatment of limbal stem cell deficiency. *Drug discovery today* **18**, 79-86 (2013).
33. Feng Y, Borrelli M, Reichl S, Schrader S, Geerling G. Review of Alternative Carrier Materials for Ocular Surface Reconstruction. *Current Eye Research* **39**, 541-552 (2014).
34. Saettone MF, Salminen L. Ocular inserts for topical delivery. *Advanced Drug Delivery Reviews* **16**, 95-106 (1995).
35. Choi SW, Kim J. Therapeutic Contact Lenses with Polymeric Vehicles for Ocular Drug Delivery: A Review. *Materials (Basel, Switzerland)* **11**, 1125 (2018).
36. Gulsen D, Chauhan A. Ophthalmic Drug Delivery through Contact Lenses. *Investigative Ophthalmology & Visual Science* **45**, 2342-2347 (2004).
37. Hui A. Contact lenses for ophthalmic drug delivery. *Clinical and Experimental Optometry* **100**, 494-512 (2017).
38. Maulvi FA, Soni TG, Shah DO. A review on therapeutic contact lenses for ocular drug delivery. *Drug Delivery* **23**, 3017-3026 (2016).
39. Karki S, Kim H, Na S-J, Shin D, Jo K, Lee J. Thin films as an emerging platform for drug delivery. *Asian Journal of Pharmaceutical Sciences* **11**, 559-574 (2016).
40. Xu KP, Tsubota K. Correlation of tear clearance rate and fluorophotometric assessment of tear turnover. *British Journal of Ophthalmology* **79**, 1042 (1995).
41. Kwatra D, Mitra AK. Drug delivery in ocular diseases: Barriers and strategies. *World Journal of Pharmacology* **2**, 78-83 (2013).
42. Bachu RD, Chowdhury P, Al-Saedi ZHF, Karla PK, Boddu SHS. Ocular Drug Delivery Barriers-Role of Nanocarriers in the Treatment of Anterior Segment Ocular Diseases. *Pharmaceutics* **10**, 28 (2018).

43. Yi X-j, Wang Y, Yu F-SX. Corneal Epithelial Tight Junctions and Their Response to Lipopolysaccharide Challenge. *Investigative Ophthalmology & Visual Science* **41**, 4093-4100 (2000).
44. Srinivasan B, Kolli AR, Esch MB, Abaci HE, Shuler ML, Hickman JJ. TEER measurement techniques for in vitro barrier model systems. *Journal of laboratory automation* **20**, 107-126 (2015).
45. Gunda S, Hariharan S, Mandava N, Mitra AK. Barriers in Ocular Drug Delivery. In: *Ocular Transporters In Ophthalmic Diseases And Drug Delivery: Ophthalmology Research* (ed<sup>^</sup>(eds Tombran-Tink J, Barnstable CJ). Humana Press (2008).
46. Smart JD. The basics and underlying mechanisms of mucoadhesion. *Advanced Drug Delivery Reviews* **57**, 1556-1568 (2005).
47. Boddupalli BM, Mohammed ZNK, Nath RA, Banji D. Mucoadhesive drug delivery system: An overview. *Journal of advanced pharmaceutical technology & research* **1**, 381-387 (2010).
48. Shaikh R, Raj Singh TR, Garland MJ, Woolfson AD, Donnelly RF. Mucoadhesive drug delivery systems. *Journal of pharmacy & bioallied sciences* **3**, 89-100 (2011).
49. Sandri G, Rossi S, Ferrari F, Bonferoni MC, Caramella CM. Mucoadhesive Polymers as Enabling Excipients for Oral Mucosal Drug Delivery. In: *Oral Mucosal Drug Delivery and Therapy* (ed<sup>^</sup>(eds Rathbone MJ, Senel S, Pather I). Springer US (2015).
50. Ohta M, Morita Y, Yamada N, Nishida T, Morishige N. Remodeling of the Corneal Epithelial Scaffold for Treatment of Persistent Epithelial Defects in Diabetic Keratopathy. *Case Reports in Ophthalmology* **9**, 333-340 (2018).
51. Bikbova G, Oshitari T, Baba T, Yamamoto S. Neuronal Changes in the Diabetic Cornea: Perspectives for Neuroprotection. *BioMed research international* **2016**, 5140823-5140823 (2016).
52. Guo C, *et al.* Intranasal delivery of nanomicelle curcumin promotes corneal epithelial wound healing in streptozotocin-induced diabetic mice. *Scientific reports* **6**, 29753-29753 (2016).
53. McLaughlin PJ, Sassani JW, Klocek MS, Zagon IS. Diabetic keratopathy and treatment by modulation of the opioid growth factor (OGF)-OGF receptor (OGFr) axis with naltrexone: a review. *Brain Res Bull* **81**, 236-247 (2010).
54. Ziaei M, Greene C, Green CR. Wound healing in the eye: Therapeutic prospects. *Adv Drug Deliv Rev* **126**, 162-176 (2018).

55. Rajak S, Rajak J, Selva D. Performing a tarsorrhaphy. *Community eye health* **28**, 10-11 (2015).
56. Xu K-P, Li Y, Ljubimov AV, Yu F-SX. High glucose suppresses epidermal growth factor receptor/phosphatidylinositol 3-kinase/Akt signaling pathway and attenuates corneal epithelial wound healing. *Diabetes* **58**, 1077-1085 (2009).
57. Kramerov AA, Saghizadeh M, Ljubimov AV. Adenoviral Gene Therapy for Diabetic Keratopathy: Effects on Wound Healing and Stem Cell Marker Expression in Human Organ-cultured Corneas and Limbal Epithelial Cells. *Journal of visualized experiments : JoVE*, e54058-e54058 (2016).
58. Wang AL, *et al.* Use of Topical Insulin to Treat Refractory Neurotrophic Corneal Ulcers. *Cornea* **36**, 1426-1428 (2017).
59. Di G, *et al.* Mesenchymal Stem Cells Promote Diabetic Corneal Epithelial Wound Healing Through TSG-6–Dependent Stem Cell Activation and Macrophage Switch. *Investigative Ophthalmology & Visual Science* **58**, 4344-4354 (2017).
60. Kramerov AA, Ljubimov AV. Stem cell therapies in the treatment of diabetic retinopathy and keratopathy. *Exp Biol Med (Maywood)* **241**, 559-568 (2016).
61. Kinoshita S, Awamura S, Oshiden K, Nakamichi N, Suzuki H, Yokoi N. Rebamipide (OPC-12759) in the Treatment of Dry Eye: A Randomized, Double-Masked, Multicenter, Placebo-Controlled Phase II Study. *Ophthalmology* **119**, 2471-2478 (2012).
62. Rangan V, Cremonini F. Rebamipide in Functional and Organic Dyspepsia: Sometimes the Best Offense Is a Good Defense. *Dig Dis Sci* **63**, 1089-1090 (2018).
63. Arakawa T, *et al.* 15th Anniversary of Rebamipide: Looking Ahead to the New Mechanisms and New Applications. *Digestive Diseases and Sciences* **50**, S3-S11 (2005).
64. Kinoshita S, *et al.* A randomized, multicenter phase 3 study comparing 2% rebamipide (OPC-12759) with 0.1% sodium hyaluronate in the treatment of dry eye. *Ophthalmology* **120**, 1158-1165 (2013).
65. Urashima H, Takeji Y, Okamoto T, Fujisawa S, Shinohara H. Rebamipide increases mucin-like substance contents and periodic acid Schiff reagent-positive cells density in normal rabbits. *J Ocul Pharmacol Ther* **28**, 264-270 (2012).
66. Takeji Y, Urashima H, Aoki A, Shinohara H. Rebamipide Increases the Mucin-Like Glycoprotein Production in Corneal Epithelial Cells. *Journal of Ocular Pharmacology and Therapeutics* **28**, 259-263 (2012).
67. Itoh S, Itoh K, Shinohara H. Regulation of Human Corneal Epithelial Mucins by Rebamipide. *Current Eye Research* **39**, 133-141 (2014).



68. Kase S, Shinohara T, Kase M. Effect of topical rebamipide on human conjunctival goblet cells. *JAMA Ophthalmol* **132**, 1021-1022 (2014).
69. Tanaka H, Fukuda K, Ishida W, Harada Y, Sumi T, Fukushima A. Rebamipide increases barrier function and attenuates TNF $\alpha$ -induced barrier disruption and cytokine expression in human corneal epithelial cells. *The British journal of ophthalmology* **97**, 912-916 (2013).
70. Tajima K, *et al.* Rebamipide suppresses TNF- $\alpha$  production and macrophage infiltration in the conjunctiva. *Veterinary Ophthalmology* **21**, 347-352 (2018).
71. Kojima T, *et al.* The Role of 2% Rebamipide Eye Drops Related to Conjunctival Differentiation in Superoxide Dismutase-1 (Sod1) Knockout Mice. *Investigative Ophthalmology & Visual Science* **59**, 1675-1681 (2018).
72. Kashima T, Akiyama H, Miura F, Kishi S. Resolution of persistent corneal erosion after administration of topical rebamipide. *Clinical Ophthalmology* **6**, 1403-1406 (2012).
73. Hayashi Y, Toshida H, Matsuzaki Y, Matsui A, Ohta T. Persistent corneal epithelial defect responding to rebamipide ophthalmic solution in a patient with diabetes. *Int Med Case Rep J* **9**, 113-116 (2016).
74. Misra SL, Braatvedt GD, Patel DV. Impact of diabetes mellitus on the ocular surface: a review. *Clinical & Experimental Ophthalmology* **44**, 278-288 (2016).
75. Arzt E, Gorb S, Spolenak R. From micro to nano contacts in biological attachment devices. *Proceedings of the National Academy of Sciences* **100**, 10603 (2003).
76. Autumn K, *et al.* Adhesive force of a single gecko foot-hair. *Nature* **405**, 681-685 (2000).
77. Gorb SN, Sinha M, Peressadko A, Daltorio KA, Quinn RD. Insects did it first: a micropatterned adhesive tape for robotic applications. *Bioinspiration & Biomimetics* **2**, S117-S125 (2007).
78. Kim JJK, Al Thuwaini H, Almuslem M. Photolithography of SU-8 microtowers for a 100-turn, 3-D toroidal microinductor. *Micro and Nano Systems Letters* **6**, 14 (2018).
79. Martinez-Duarte R, Madou M. SU-8 Photolithography and Its Impact on Microfluidics. In: *Microfluidics and Nanofluidics Handbook* (ed<sup>^</sup>(eds) (2010).
80. Guan J, Ferrell N, James Lee L, Hansford DJ. Fabrication of polymeric microparticles for drug delivery by soft lithography. *Biomaterials* **27**, 4034-4041 (2006).
81. Qin D, Xia Y, Whitesides GM. Soft lithography for micro- and nanoscale patterning. *Nature Protocols* **5**, 491-502 (2010).

82. Perrigin JA, Morgan A, Quintero S, Perrigin D, Brown S, Bergmanson J. Comparison of pH Values of Selected Ocular Lubricants. *Investigative Ophthalmology & Visual Science* **45**, 3913-3913 (2004).
83. Macoull KL, Pavan-Langston D. Pilocarpine Ocusert System for Sustained Control of Ocular Hypertension. *Archives of Ophthalmology* **93**, 587-590 (1975).
84. Lin S-Y, Lee C-J, Lin Y-Y. The Effect of Plasticizers on Compatibility, Mechanical Properties, and Adhesion Strength of Drug-Free Eudragit E Films. *Pharmaceutical Research* **8**, 1137-1143 (1991).
85. Vaidya A, Pathak K. 17 - Mechanical stability of dental materials. In: *Applications of Nanocomposite Materials in Dentistry* (ed<sup>^</sup>(eds Asiri AM, Inamuddin, Mohammad A). Woodhead Publishing (2019).
86. Sciences PCoEaM. MATSE 81: Materials in Today's World. (ed<sup>^</sup>(eds).
87. Bhamra TS, Tighe BJ. Mechanical properties of contact lenses: The contribution of measurement techniques and clinical feedback to 50 years of materials development. *Contact Lens and Anterior Eye* **40**, 70-81 (2017).
88. MatWeb.  
Evonik EUDRAGIT® FS 30 D Copolymer. (ed<sup>^</sup>(eds).
89. Park M, Richardson A, Pandzic E, Lobo EP, Lyons JG, Di Girolamo N. Peripheral (not central) corneal epithelia contribute to the closure of an annular debridement injury. *Proceedings of the National Academy of Sciences* **116**, 26633 (2019).
90. Rampersad SN. Multiple applications of Alamar Blue as an indicator of metabolic function and cellular health in cell viability bioassays. *Sensors (Basel, Switzerland)* **12**, 12347-12360 (2012).
91. Bonnier F, *et al.* Cell viability assessment using the Alamar blue assay: A comparison of 2D and 3D cell culture models. *Toxicology in Vitro* **29**, 124-131 (2015).
92. Wu Y, *et al.* Research progress of in-situ gelling ophthalmic drug delivery system. *Asian Journal of Pharmaceutical Sciences* **14**, 1-15 (2019).
93. Uchino Y, Woodward AM, Argüeso P. Differential effect of rebamipide on transmembrane mucin biosynthesis in stratified ocular surface epithelial cells. *Experimental Eye Research* **153**, 1-7 (2016).
94. Mansuri S, Kesharwani P, Jain K, Tekade RK, Jain NK. Mucoadhesion: A promising approach in drug delivery system. *Reactive and Functional Polymers* **100**, 151-172 (2016).

95. Lee P, Shen Y, Eberle M. The long-acting Ocusert-pilocarpine system in the management of glaucoma. *Investigative Ophthalmology & Visual Science* **14**, 43-46 (1975).
96. McDonald M, D'Aversa G, Perry HD, Wittpenn JR, Donnenfeld ED, Nelinson DS. Hydroxypropyl cellulose ophthalmic inserts (lacrisert) reduce the signs and symptoms of dry eye syndrome and improve patient quality of life. *Transactions of the American Ophthalmological Society* **107**, 214-221 (2009).
97. Mishima S, Gasset A, Klyce SD, Jr., Baum JL. Determination of Tear Volume and Tear Flow. *Investigative Ophthalmology & Visual Science* **5**, 264-276 (1966).